DOCKET NO.: RFU0001-100 **PATENT**

IN THE UNITED STATES PATENT AND TRADEMARK OFFICE

In re patent application of: Jeffrey Ravetch

Serial No.: 09/834,321 **Group No.:** 1644

Filing Date: April 13, 2001 **Examiner:** Michail A Belyavskyi

For: **ENHANCEMENT OF ANTIBODY-MEDIATED IMMUNE RESPONSES**

DECLARATION OF DR. JEFFREY V. RAVETCH
PURSUANT TO 37 CFR § 1.132

I, Dr. Jeffrey V. Ravetch , declare as follows:

1. I am an inventor in the above-identified patent application.

2. I am familiar with the Shields reference (*Journal of Biological Chemistry*, Vol. 276, No. 9, pp. 6591-6604 (2001)) entitled "High Resolution Mapping of the Binding Site on Human IgG1 for FcγRI, FcγRII, FcγRIII, and FcRn and Design of IgG1 Variants with Improved Binding to the FcγR," (a copy of which is attached hereto).

3. In the experiments described therein, antibodies that have reduced binding affinity to FcγRIIB were produced and the data is reported on Tables I - III. The antibodies were produced by site-directed mutagenesis and screening methods to determine if the binding is reduced to FcγRIIB.

Dated: 8/17/06

By: _____

Dr. Jeffrey V. Ravetch

THE JOURNAL OF BIOLOGICAL CHEMISTRY
Vol. 276, No. 9, Issue of March 2, pp. 6591–6604, 2001
Printed in U.S.A.

High Resolution Mapping of the Binding Site on Human IgG1 for FcγRI, FcγRII, FcγRIII, and FcRn and Design of IgG1 Variants with Improved Binding to the FcγR*

Received for publication, October 17, 2000
Published, JBC Papers in Press, November 28, 2000, DOI 10.1074/jbc.M009483200

Robert L. Shields‡, Angela K. Namenuk‡, Kyu Hong§, Y. Gloria Meng§, Julie Rae‡, John Briggs¶, Dong Xie‖, Jadine Lai‡, Andrew Stadlen‡, Betty Li‡, Judith A. Fox‖, and Leonard G. Presta‡**

From the ‡Department of Immunology, the §Department of BioAnalytical Technology, the ¶Department of Analytical Chemistry, and the ‖Department of Pharmacokinetics and Metabolism, Genentech, Inc., South San Francisco, California 94080

Immunoglobulin G (IgG) Fc receptors play a critical role in linking IgG antibody-mediated immune responses with cellular effector functions. A high resolution map of the binding site on human IgG1 for human FcγRI, FcγRIIA, FcγRIIB, FcγRIIIA, and FcRn receptors has been determined. A common set of IgG1 residues is involved in binding to all FcγR; FcγRII and FcγRIII also utilize residues outside this common set. In addition to residues which, when altered, abrogated binding to one or more of the receptors, several residues were found that improved binding only to specific receptors or simultaneously improved binding to one type of receptor and reduced binding to another type. Select IgG1 variants with improved binding to FcγRIIIA exhibited up to 100% enhancement in antibody-dependent cell cytotoxicity using human effector cells; these variants included changes at residues not found at the binding interface in the IgG/FcγRIIIA co-crystal structure (Sondermann, P., Huber, R., Oosthuizen, V., and Jacob, U. (2000) *Nature* 406, 267–273). These engineered antibodies may have important implications for improving antibody therapeutic efficacy.

Monoclonal antibodies (mAbs)[1] are increasingly being used as therapeutics in human disease (1–3). Although some of these, *e.g.* mAbs that bind to a receptor or ligand and thereby block ligand-receptor interaction, may function without utilizing antibody effector mechanisms, other mAbs may need to recruit the immune system to kill the target cell (4–6). If immune system recruitment is desirable for a therapeutic mAb, engineering the IgG Fc portion to improve effector function (via improved binding to IgG receptors and/or complement) could be a valuable enhancement to antibody therapeutics. Currently, immune system recruitment can be abrogated by altering IgG residues in the lower hinge region (7, 8), using human IgG2 or IgG4 subclasses that are comparatively inefficient in effector function or using antibody F(ab) or $F(ab')_2$ fragments (although these may have undesirable rapid clearance rates). There are few methods that improve immune system recruitment; these include bispecific antibodies, in which one arm of the antibody binds to an IgG receptor (9), cytokine-IgG fusion proteins (10), and optimization of the Asn^{297}-linked carbohydrate (11, 12). Alteration of clearance rate is also being investigated (13).

IgG Fc receptors play a critical role in linking IgG antibody-mediated immune responses with cellular effector functions. The latter include release of inflammatory mediators, endocytosis of immune complexes, phagocytosis of microorganisms, antibody-dependent cellular cytotoxicity (ADCC), and regulation of immune system cell activation (14–17). One group of IgG Fc receptors, FcγR, are expressed on leukocytes and are composed of three distinct classes as follows: FcγRI (CD64), FcγRII (CD32), and FcγRIII (CD16). In humans, the latter two classes can be further divided into FcγRIIA and FcγRIIB, FcγRIIIA and FcγRIIIB. Structurally, the FcγR are all members of the immunoglobulin superfamily, having an IgG-binding α-chain with an extracellular portion composed of either two (FcγRII and FcγRIII) or three (FcγRI) Ig-like domains. In addition, FcγRI and FcγRIII have accessory protein chains (γ and ζ) associated with the α-chain that function in signal transduction. The receptors are also distinguished by their affinity for IgG. FcγRI exhibits a high affinity for IgG, $K_a = 10^8$–10^9 M^{-1} (14), and can bind monomeric IgG. In contrast, FcγRII and FcγRIII show a weaker affinity for monomeric IgG, $K_a \leq 10^7$ M^{-1} (14), and hence can only interact effectively with multimeric immune complexes.

Given the interest in and increasing use of antibody therapeutics, a comprehensive mapping of the binding site on human IgG for the different FcγR could provide for alternative methods of either abrogating or enhancing immune recruitment via FcγR. Previous studies mapped the binding site on human and murine IgG for FcγR primarily to the lower hinge region composed of IgG residues 233–239 (Eu numbering, see Ref. 18) (8, 14–17, 19–22). Other studies proposed additional broad segments, *e.g.* Gly^{316}–Lys^{338} for human FcγRI (21), Lys^{274}–Arg^{301} and Tyr^{407}–Arg^{416} for human FcγRIII (23, 24), or found few specific residues outside the lower hinge, *e.g.* Asn^{297} and Glu^{318} for murine IgG2b interacting with murine FcγRII (25). The very recent report of the 3.2-Å crystal structure of the human IgG1 Fc fragment with human FcγRIIIA

* The costs of publication of this article were defrayed in part by the payment of page charges. This article must therefore be hereby marked "*advertisement*" in accordance with 18 U.S.C. Section 1734 solely to indicate this fact.

** To whom correspondence should be addressed: Dept. of Immunology, MS 34, Genentech, Inc., 1 DNA Way, South San Francisco, CA 94080. E-mail: presta@gene.com.

[1] The abbreviations used are: mAb, monoclonal antibody; ADCC, antibody-dependent cell cytotoxicity; AICC, antibody-independent cell cytotoxicity; ELISA, enzyme-linked immunosorbent assay; FcγR, IgG Fc γ-receptor; FcRn, neonatal IgG Fc receptor; GST, human glutathione *S*-transferase; LDH, lactate dehydrogenase; MR, maximal response; NK, natural killer cells; PBMC, peripheral blood monocytes; PE, (*R*)-phycoerythrin; SR, spontaneous release; VEGF, vascular endothelial growth factor; PCR, polymerase chain reaction; MALDI-TOF-MS, matrix-assisted laser desorption/ionization time-of-flight mass spectrometry; CHO, Chinese hamster ovary; PBS, phosphate-buffered saline; BSA, bovine serum albumin.

delineated IgG1 residues Leu^{234}–Ser^{239}, Asp^{265}–Glu^{269}, Asn^{297}–Thr^{299}, and Ala^{327}–Ile^{332} as involved in binding to FcγRIIIA (26).

The current study provides a complete, high resolution mapping of human IgG1 for human FcγR receptors (FcγRI, FcγRIIA, FcγRIIB, and FcγRIIIA) as well as for human FcRn, an Fc receptor belonging to the major histocompatability complex structural class, which is involved in IgG transport and clearance (27, 28). The binding site on human IgG1 for the various receptors was determined by individually changing all solvent-exposed amino acids in human IgG1 CH2 and CH3 domains, based on the crystal structure of human IgG1 Fc (30), to Ala. A common set of IgG1 residues is involved in binding to all FcγR; FcγRII and FcγRIII also utilize distinct residues in addition to this common set. As well as residues that abrogated binding to one or more Fc receptors when changed to Ala, several positions were found that improved binding only to specific receptors or simultaneously improved binding to one type of FcγR and reduced binding to another type. Notably, for both FcγRIIIA and FcRn, which have crystal structures of complexes with IgG available (26, 29), several IgG residues not found at the IgG:receptor interface had a profound effect on binding and biological activity. Select IgG1 variants with improved binding to FcγRIIIA showed an enhancement in ADCC when either peripheral blood monocyte cells (PBMC) or natural killer cells (NK) were used. These variants may have important implications for using Fc-engineered antibodies for improved therapeutic efficacy.

EXPERIMENTAL PROCEDURES

cDNA Constructs and Soluble Receptor Expression—The cDNAs encoding extracellular and transmembrane domains of human FcγRIIA (CD32A; His^{131} allotype), FcγRIIB (CD32B), and FcγRIIIA (CD16A; Val^{158} allotype) were provided by Dr. J. Ravetch (Rockefeller University, New York). FcγRIIA-Arg^{131} allotype and FcγRIIIA-Phe^{158} allotype were generated by site-directed mutagenesis (31). The cDNA for FcγRI (CD64) was isolated by reverse transcriptase-PCR (GeneAmp, PerkinElmer Life Sciences) of oligo(dT)-primed RNA from U937 cells using primers that generated a fragment encoding the α-chain extracellular domain. The cDNAs encoding human neonatal Fc receptor (FcRn) α-chain, β_2-microglobulin subunit, and human FcγR γ-chain were obtained from the I.M.A.G.E. Consortium (32). The coding regions of all receptors were subcloned into previously described pRK mammalian cell expression vectors (33).

For all FcγR and the FcRn α-chain pRK plasmids, the transmembrane and intracellular domains were replaced by DNA encoding a $Gly\text{-}His_6$ tag and human glutathione *S*-transferase (GST). The 234-amino acid GST sequence was obtained by PCR from the pGEX-4T2 plasmid (Amersham Pharmacia Biotech) with *Nhe*I and *Xba*I restriction sites at the 5′ and 3′ ends, respectively. Thus, the expressed proteins contained the extracellular domains of the α-chain fused at their carboxyl termini to Gly/His_6/GST at amino acid positions as follows: FcγRI, His^{292}; FcγRIIA, Met^{216}; FcγRIIB, Met^{196}; FcγRIIIA, Gln^{191}; FcRn, Ser^{297} (residue numbers include signal peptides).

Plasmids were transfected into the adenovirus-transformed human embryonic kidney cell line 293 by calcium phosphate precipitation (34). Supernatants were collected 72 h after conversion to serum-free PSO_4 medium supplemented with 10 mg/liter recombinant bovine insulin, 1 mg/liter human transferrin, and trace elements. Proteins were purified by nickel-nitrilotriacetic acid chromatography (Qiagen, Valencia, CA) and buffer exchanged into phosphate-buffered saline (PBS) using Centriprep-30 concentrators (Millipore, Bedford, MA). Proteins were analyzed on 4–20% SDS-polyacrylamide gels (NOVEX, San Diego, CA), transferred to polyvinylidene difluoride membranes (NOVEX), and their amino termini sequenced to ensure proper signal sequence cleavage. Receptor conformation was evaluated by ELISA using murine monoclonals 32.2 (anti-FcγRI), IV.3 (anti-FcγRII), 3G8 (anti-FcγRIII) (Medarex, Annandale, NJ), and B1G6 (anti-β_2-microglobulin) (Beckman Coulter, Palo Alto, CA). Receptor concentrations were determined by amino acid analysis.

Human IgG1 Mutagenesis—The humanized IgG1 anti-IgE E27, an affinity-matured variant of anti-IgE E25, binds to the Fcε3 domain of human IgE (35). When mixed with human IgE in a 1:1 molar ratio, the IgE and anti-IgE form a hexameric complex composed of three IgE and three anti-IgE (36). Site-directed mutagenesis (31) on E27 IgG1 was used to generate IgG1 variants in which all solvent-exposed residues in the CH2 and CH3 domains were individually altered to Ala; selection of solvent-exposed residues was based on the crystal structure of human IgG1 Fc (30). Human IgG2, IgG3, and IgG4 isotypes of E27 were constructed by subcloning the appropriate heavy chain Fc cDNAs from a human spleen cDNA library into a pRK vector containing the E27 variable heavy domain. All IgG isotypes and variants were expressed using the same E27 κ light chain.

Following cotransfection of heavy and light chain plasmids into 293 cells, IgG1, IgG2, IgG4, and variants were purified by protein A chromatography (Amersham Pharmacia Biotech). IgG3 isotype was purified using protein G chromatography (Amersham Pharmacia Biotech). All proteins were analyzed by SDS-polyacrylamide gel electrophoresis. Protein concentrations were determined using A_{280} and verified using amino acid composition analysis and a human IgG Fc ELISA. IgGs were also tested for their binding to human IgE in an ELISA format to ensure that they bound IgE as well as native E27. Structural integrity of the variants was also evident by their ability to be purified using protein A (which binds at the CH2:CH3 domain interface (30)) as well as all variants, except P329A, binding similar to native IgG1 to at least one of the five receptors.

IgG Immune Complexes and IgG Binding to FcγR—FcγRIIA, FcγRIIB, and FcγRIIIA fusion proteins at 1 μg/ml in PBS, pH 7.4, were coated onto ELISA plates (Nalge-Nunc, Naperville, IL) for 48 h at 4 °C. Plates were blocked with Tris-buffered saline, 0.5% bovine serum albumin, 0.05% polysorbate-20, 2 mM EDTA, pH 7.45 (assay buffer), at 25 °C for 1 h. E27-IgE hexameric complexes were prepared in assay buffer by mixing equimolar amounts of E27 and human myeloma IgE (37) at 25 °C for 1 h. Serial 3-fold dilutions of native E27 standard or variant complexes (10.0–0.0045 μg/ml) were added to plates and incubated for 2 h. After washing plates with assay buffer, bound complexes to FcγRIIA and FcγRIIB were detected with peroxidase-conjugated $F(ab')_2$ fragment of goat anti-human $F(ab')_2$-specific IgG (Jackson ImmunoResearch, West Grove, PA). Binding of complexes to FcγRIIIA was detected with peroxidase-conjugated protein G (Bio-Rad). The substrate used was *o*-phenylenediamine dihydrochloride (Sigma). Absorbance at 490 nm was read using a V_{max} plate reader (Molecular Devices, Mountain View, CA). Any contribution to binding via interaction of the IgE in the E27-IgE complexes with the human FcγRII and FcγRIIIA was not apparent based on the lack of binding of several Ala variants (Class 1, Table I).

For the high affinity FcγRI, the receptor fusion protein at 1.5 μg/ml in PBS, pH 7.4, was coated onto ELISA plates (Nunc) for 18 h at 4 °C. Plates were blocked with assay buffer at 25 °C for 1 h. Serial 3-fold dilutions of monomeric E27 and variants (10.0–0.0045 μg/ml) were added to plates and incubated for 2 h. After washing plates with assay buffer, IgG bound to FcγRI was detected with peroxidase-conjugated $F(ab')_2$ fragment of goat anti-human $F(ab')_2$-specific IgG (Jackson ImmunoResearch) or with peroxidase-conjugated protein G (Bio-Rad). The substrate used was *o*-phenylenediamine dihydrochloride (Sigma). Absorbance at 490 nm was read using a V_{max} plate reader (Molecular Devices).

For all FcγR, binding values reported are the binding of each E27 variant relative to native E27, taken as $(A_{490\ nm(variant)}/A_{490\ nm(native\ IgG1)})$ at 0.33 or 1 μg/ml for FcγRII and FcγRIIIA and 2 μg/ml for FcγRI. A value greater than 1 denotes binding of the variant was improved compared with native IgG1, whereas a ratio less than 1 denotes reduced binding compared with native IgG1. Reduced binding to any given receptor was defined as a reduction of ≥40% compared with native IgG; better binding was defined as an improvement of ≥25% compared with native IgG1. The latter was chosen based on the observation that variants with ≥25% improved binding in the ELISA format assay, such as E333A, K334A, and S298A, also showed improved efficacy in the cell-based binding and ADCC assays.

IgG Binding to FcRn—ELISA plates (Nunc) were coated with 2 μg/ml NeutrAvidin (Pierce) or streptavidin (Zymed Laboratories Inc., South San Francisco, CA) in 50 mM carbonate buffer, pH 9.6, at 4 °C overnight (the same results were obtained with either molecule). Plates were blocked with PBS, 0.5% BSA, 10 ppm Proclin 300 (Supelco, Bellefonte, PA), pH 7.2, at 25 °C for 1 h. FcRn-$Gly\text{-}His_6$-GST was biotinylated using a standard protocol with biotin-X-NHS (Research Organics, Cleveland, OH) and bound to NeutrAvidin-coated plates at 2 μg/ml in PBS, 0.5% BSA, 0.05% polysorbate-20 (sample buffer), pH 7.2, at 25 °C for 1 h. Plates were then rinsed with sample buffer, pH 6.0. Eight serial 2-fold dilutions of E27 standard or variants (1.6–200 ng/ml) in sample buffer at pH 6.0 were incubated for 2 h. Plates were rinsed with sample buffer,

pH 6.0, and bound IgG was detected with peroxidase-conjugated goat $F(ab')_2$ anti-human IgG $F(ab')_2$ (Jackson ImmunoResearch) in pH 6.0 sample buffer using 3,3',5,5'-tetramethylbenzidine (Kirkegaard & Perry Laboratories, Gaithersburg, MD) as substrate. Absorbance at 450 nm was read on a V_{max} plate reader (Molecular Devices). Titration curves were analyzed by a four-parameter nonlinear regression fit (KaleidaGraph, Synergy Software, Reading, PA). For each ELISA plate assay, a full titration curve of E27 standard was done. The absorbance at the midpoint of the titration curve (mid-OD) and its corresponding E27 concentration were determined. Then the concentration of each variant at this mid-OD was determined, and the concentration of E27 was divided by the concentration of each variant. Hence, the values are a ratio of the binding of each variant relative to native IgG1 standard. A control human IgG1 was run on each ELISA plate as a control and had a ratio of 1.12 ± 0.07 (n = 92).

A second format was also evaluated in which IgE was coated on plates instead of the FcRn. MaxiSorp 96-well microwell plates (Nunc) were coated with 1 μg/ml IgE in 50 mM carbonate buffer, pH 9.6, at 4 °C overnight. Plates were blocked with PBS, 0.5% bovine serum albumin, 10 ppm Proclin 300, pH 7.2, at 25 °C for 1 h. 2-fold serial dilutions of anti-IgE antibodies (1.6–200 ng/ml) in PBS, 0.5% BSA, 0.05% polysorbate 20, pH 6.0 (sample buffer), were added to the plates, and plates were incubated for 2 h at 25 °C. Biotinylated FcRn at 3.6 μg/ml in sample buffer was added to the plates. After a 1-h incubation, bound FcRn was detected by adding streptavidin-labeled peroxidase (Amdex, Copenhagen, Denmark) in sample buffer, incubating the plates for 1 h and adding 3,3',5,5'-tetramethylbenzidine as the substrate. Plates were washed between steps with PBS, 0.5% BSA, 0.05% polysorbate 20, pH 6.0. Absorbance was read at 450 nm on a V_{max} plate reader, and titration curves were fit as described above.

IgG Binding to Cell-bound FcγR—The expression of FcγRI on THP-1 cells (38) was confirmed using the anti-FcγRI antibody 32.2 (Medarex). Binding of IgG to FcγRI on THP-1 cells was performed by incubating monomeric IgG in staining buffer (PBS, 0.1% BSA, 0.01% sodium azide) with 5 × 10^5 cells/well in 96-well round-bottom tissue culture plates (Costar, Cambridge, MA) at 4 °C for 30 min. Cells were washed three times with staining buffer, and IgG binding was detected by addition of 1:200 fluorescein isothiocyanate-$F(ab')_2$ fragment of goat anti-human F(ab')2 specific for human IgG (Jackson ImmunoResearch). Immunofluorescence staining was analyzed on a FACScan flow cytometer using Cellquest software (Becton Dickinson, San Jose, CA). Dead cells were excluded from analysis by the addition of 1 μg/ml propidium iodide.

The CHO stable cell lines expressing FcγRIIIA-Phe^{158} and FcγRIIIA-Val^{158} with human γ-chain were generated by subcloning the α-chain and γ-chains into a previously described vector that includes DNA encoding a green fluorescent protein (39). CHO cell transfection was carried out using Superfect (Qiagen) according to the manufacturer's instructions. Fluorescence-activated cell sorting was done based on green fluorescent protein expression as described previously (40). Receptor expression levels were determined by staining with anti-FcγRIII monoclonal antibody 3G8 (Medarex). Binding of IgG1 variants was performed by adding monomeric IgG in staining buffer to 5 × 10^5 cells and incubating in 96-well round-bottom tissue culture plates (Costar, Cambridge, MA) at 4 °C for 30 min. Cells were washed three times with staining buffer, and IgG binding was detected by addition of 1:200 PE-$F(ab')_2$ fragment of goat anti-human IgG and incubation for 30 min at 4 °C. After washing, immunofluorescence staining was analyzed on a FACScan flow cytometer using Cellquest software (Becton Dickinson). Dead cells were excluded from analysis by addition of 1 μg/ml propidium iodide.

MALDI Analysis of Released N-Linked Oligosaccharides—To determine whether differences in binding among variants was related to variation in the oligosaccharide at the conserved Asn^{297}-linked glycosylation site, oligosaccharides of various IgG variants were analyzed using matrix-assisted laser desorption/ionization time-of-flight mass spectrometry (MALDI-TOF-MS) as described previously (41). Following immobilization of ~50 μg of IgG to polyvinylidene difluoride membranes in 96-well MultiScreen IP plates (Millipore), proteins were reduced with 50 μl of 0.1 M dithiothreitol in 8 M urea, 360 mM Tris, 3.2 mM EDTA, pH 8.6 (RCM buffer). Resultant free sulfhydryl groups were subsequently carboxymethylated by incubation with 0.1 M iodoacetic acid in RCM buffer at 25 °C for 30 min in the dark. Prior to enzymatic release of glycoproteins, membrane-bound proteins were incubated in 1% aqueous polyvinylpyrrolidone 360 (Sigma) solution at 25 °C for 1 h. Oligosaccharides were released by incubating protein with 32 units of peptide:N-glycosidase F (New England Biolabs, Beverly, MA) in 25 μl of Tris acetate buffer, pH 8.4, at 37 °C for 3 h, followed by acidification by addition of 2.5 μl of 1.5 M acetic acid and then incubated for 25 °C for 3 h. Samples were then purified by cation exchange chromatography using hydrogen form, 100–200 mesh AG50W-X8 resin (Bio-Rad). Released oligosaccharides were analyzed by MALDI-TOF-MS in both positive and negative modes using matrices containing 2,5-dihydroxybenzoic acid and 2,4,6-trihydroxyacetophenone, respectively (42). Analysis was performed on a Voyager DE mass spectrometer (Perspective Biosystems, Foster City, CA) by transferring 0.5 μl of sample to a stainless steel target containing 0.4 μl of the appropriate matrix. Following vacuum dessication, the samples were ionized by irradiation with an N2 laser (337 nm wavelength), and ions were accelerated with a 20-kV voltage. Ion mass assignment was made using oligosaccharide standards (Oxford Glycosciences, Rosedale, NY) in a two-point external calibration. Final spectra were the result of the summation of the individual spectral data from 240 laser ignitions.

ADCC Assays Using PBMC as Effector Cells—SK-BR-3 (ATCC HTB-30) breast tumor cell line expressing p^{185}HER2 (43) as target cell was purchased from the American Type Culture Collection. Effector cells were PBMC purified from four healthy donors using Lymphocyte Separation Medium (LSM, Organon Technika, Durham, NC) on the day of the experiment. ADCC was conducted by measuring the lactate dehydrogenase (LDH) activity released from the dead or plasma membrane damaged cells. SK-BR-3 (target) cells were detached from plates using Versene (Life Technologies, Inc.), washed three times with RPMI 1640 medium (Life Technologies, Inc.), and incubated with humanized anti-p^{185}HER2 IgG1 HERCEPTIN® (44) at 1 μg/ml (maximum ADCC) or 2 ng/ml for 30 min at 25 °C. HERCEPTIN® IgG variants were evaluated only at 2 ng/ml. Purified PBMC effector cells were washed three times with medium and placed in 96-well U-bottom Falcon plates (Becton Dickinson) using 2-fold serial dilution from 3 × 10^5 cells/well (100:1 effector/target ratio) to 600 cells/well (0.2:1). Opsonized SK-BR-3 cells were added to each well at 3 × 10^3 cells/well. AICC was measured by adding effector and target cells without antibody. Spontaneous release (SR, negative control) was measured by adding only target or effector cells; maximum release (MR, positive control) was measured by adding 2% Triton X-100 to target cells. After 4 h of incubation at 37 °C in 5% CO_2, assay plates were centrifuged. The supernatant was transferred to a 96-well flat-bottom Falcon plates and incubated with LDH reaction mixture (LDH Detection Kit, Roche Molecular Biochemicals) for 30 min at 25 °C. The reaction was stopped by adding 50 μl of 1 N HCl. The samples were measured at 490 nm with reference wavelength of 650 nm. The percent cytotoxicity was calculated as $((\text{LDH release}_{sample} - SR_{effector} - SR_{target})/(MR_{target} - SR_{target})) \times 100$. For each assay and antibody, the percent cytotoxicity *versus* log(effector/target ratio) was plotted and the area under the curve (AUC) calculated.

ADCC Assays Using NK as Effector Cells—FcγRIIIA allotype of human donors was determined using a previously reported two-step PCR of genomic DNA (45). Following LSM (Cappel-ICN, Aurora, OH) purification of whole blood PBMCs, NK cells were purified by negative selection using a magnetic bead NK cell isolation kit (Miltenyi Biotech, Auburn, CA) and suspended in 50:50 Ham's F-12/Dulbecco's modified Eagle's medium (Life Technologies, Inc.) containing 1% heat-inactivated fetal bovine serum (HyClone, Logan, UT), 1% penicillin/streptomycin (Life Technologies, Inc.), 2 mM L-glutamine, 0.01 M HEPES buffer. Cell purity was assessed by staining with PE-conjugated anti-CD56 and PE-conjugated anti-CD16 (PharMingen, San Diego, CA). SK-BR-3 cells were opsonized with 1 ng/ml of either native or variant humanized anti-p^{185}HER2 IgG1 HERCEPTIN® for 30 min at 25 °C in 50:50 Ham's F-12/Dulbecco's modified Eagle's medium in sterile 96-well round-bottom plates. Serial 2-fold dilutions of NK cells were added to provide a final effector/target ratio ranging from 10:1 to 0.156:1. The plates were incubated for 4 h at 37 °C in a humidified 5% CO_2 incubator. Cytotoxicity of targets was measured by LDH release using the colorimetric LDH Detection Kit (Roche Molecular Biochemicals). Spontaneous release (SR) was measured in wells with target and effector cells only; maximal release (MR) was measured by addition of 1% Triton X-100 detergent to control wells. Percent cytotoxicity was expressed as $(\text{LDH release}_{sample}/MR) \times 100$.

RESULTS

Binding of IgG Subclasses to FcγR—IgG1 binding to FcγRI is of sufficient affinity to allow detection of monomeric IgG1. In contrast, monomeric IgG1 does not bind well to FcγRII and FcγRIII, and these receptors require a multimeric complex for assay. Previous studies investigating FcγRII and FcγRIII have utilized rosetting assays (46, 47), heat-denatured (aggregated) IgG1 binding (48, 49), and dimeric IgG (46, 47, 50). In this

The Journal of Biological Chemistry

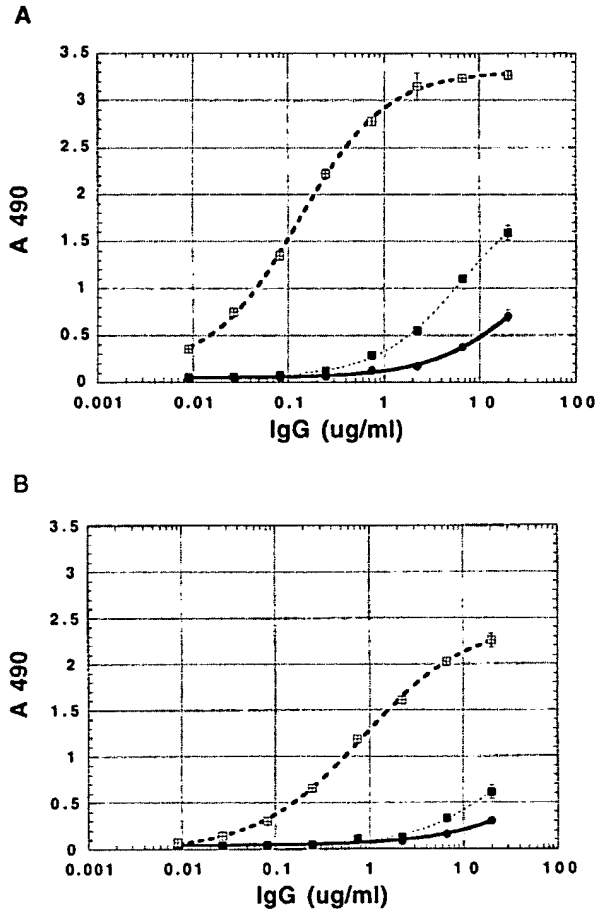

FIG. 1. **Binding of anti-IgE E27 IgG1 to human FcγR.** *A*, binding of E27 monomers (*solid circles*), dimeric (*solid squares*), and hexameric (*open squares*) complexes to FcγRIIA-Arg^{131}. *B*, binding of E27 monomers (*solid circles*), dimeric (*solid squares*), and hexameric (*open squares*) complexes to FcγRIIIA-Phe^{158}. Dimers were formed by mixing E27 IgG1 and a F(ab')$_2$ fragment of goat anti-human κ light chain at 1:0.5 molar ratio at 25 °C for 1 h (50). Hexameric complexes (*i.e.* trimeric in E27 IgG1) were formed by mixing E27 IgG1 with human IgE in a 1:1 molar ratio at 25 °C for 1 h (36).

study, a stable hexameric immune complex composed of three IgE and three anti-IgE molecules (36) was used to evaluate IgG1 binding to FcγRII and FcγRIII. Fig. 1 shows that these complexes bind to FcγRII and FcγRIII in a concentration-dependent, saturable manner.

To ensure that the results of binding of the IgE-anti-IgE hexamer complexes were not an idiosyncratic feature of the anti-IgE IgG1, complexes composed of VEGF and anti-VEGF IgG1 were also assayed for selected variants. These complexes were formed by mixing human VEGF and humanized anti-VEGF (51) in a 1:1 molar ratio. These complexes have not been fully characterized as to their size, but sedimentation ultracentrifugation experiments show that they form octamers (four VEGF:four anti-VEGF) and larger.[2] The pattern of binding for the variants was the same regardless of whether the IgE-anti-IgE or VEGF-anti-VEGF complexes were used (data not shown).

The relative affinities of human IgG subclasses IgG1, IgG2, IgG3, and IgG4 and of murine subclasses IgG1, IgG2a, and IgG2b to the FcγR have been previously determined (14–16). The pattern of binding of human and murine subclasses to human FcγRI, FcγRIIA, and FcγRIIIA was verified using the ELISA format assays (data not shown). Human FcγRIIA has two known, naturally occurring allotypes that are determined by the amino acid at position 131 (52). In this study, the FcγRIIA-Arg^{131} allotype was primarily used, but some IgG variants were tested against the FcγRIIA-His^{131} form. Human FcγRIIIA has naturally occurring allotypes at position 48 (Leu, His, or Arg) and at position 158 (Val or Phe). For the FcγRIIIA assays in this study, the FcγRIIIA-Arg^{48}/Phe^{158} allotype was used. Binding to the FcγRIIIA-Arg^{48}/Val^{158} allotype was also evaluated for selected variants.

To ensure that the results from the ELISA format assays reflected binding to FcγR on cells, selected variants were tested in cell-based assays. The binding of variants to THP-1 cells, which express FcγRI, was the same as for the ELISA-based assays; indeed, for FcγRI the cell-based results were included in the mean values cited in Table I. For FcγRIIIA, a select panel of variants was assayed on a stable-transfected CHO cell line expressing human FcgRIIIA-Phe^{158} (α- and γ-chains) and the pattern of binding reflected that found in the ELISA-based format (data not shown).

Segregation of Individual Variants into Classes—The IgG1 variants can be separated into distinct classes based on their effects on binding to the various receptors. Class 1 consists of variants that showed reduced binding to all FcγR (Table I) and are clustered near the region of the CH2 domain where the hinge joins CH2 (Fig. 2*A*). In the E233P/L234V/L235A/G236deleted variant, part of the so-called lower hinge region (residues 233–239) of human IgG1 was exchanged with that of human IgG2. The reduction in binding to all FcγR is in agreement with previous studies (8, 19, 21, 22, 25, 53, 54); this variant also showed impaired binding to FcRn. Two other residues in the lower hinge region were individually changed to Ala; P238A (Class 1) had a more pronounced effect than S239A (Class 8). If the P238A effect is due to a conformation change, this change was beneficial for binding to FcRn. In contrast, P329A showed a relatively modest reduction in binding to FcRn compared with the significant reduction in binding to the FcγR. In the IgG1 Fc:FcγRIIIA crystal structure (26), Pro^{329} intimately interacts with two Trp side chains of the receptor, and the loss of these interactions by P329A may account for the severe reduction in binding. Pro^{329} is also involved in binding of human IgG1 to human C1q (55).

Removal of the conserved Asn-linked glycosylation site in the CH2 domain, N297A, abolished binding, in agreement with earlier studies (56, 57). Another residue that interacts with carbohydrate, Asp^{265}, has also been found previously to be important in human IgG3 binding to human FcγRI (56, 57). In human IgG1, changing Asp^{265} to Ala, Asn, or Glu nullified binding (Tables I and II), suggesting that both the charge and size are important. The results of the A327Q (Class 1) and A327S (Class 2) variants imply that the region around Ala^{327} involved in binding to the FcγR may require a close fit between receptor and IgG1, as enlarging this side chain diminished binding. This position is an Asp in mouse IgG2a and IgG2b, and therefore changing the human IgG1 Ala to a larger side chain is unlikely to have affected the conformation. The A327G (Class 8) variant reduced binding only to FcγRIIIA suggesting that this receptor requires the presence of a small amino acid side chain at this position, whereas the other receptors do not.

Class 1 variants (in addition to the hinge residues, which were not investigated in this study) compose the entire binding site on IgG1 for FcγRI. Residues in the F(ab) portions of the IgG1 do not contribute to FcγRI binding as evidenced by both a CD4-immunoadhesin (58) and an Fc fragment binding to FcγRI as effectively as did intact IgG1 (data not shown). Notably, no variants were found that reduced binding only to FcγRI.

[2] J. Liu and S. Shire, personal communication.

TABLE I
Binding of human IgG1 variants to human FcRn and FcγR

Variant[a]	FcRn[b] mean (S.D.) *n*	FcγRI mean (S.D.) *n*	FcγRIIA mean (S.D.)	FcγRIIB mean (S.D.)	FcγRIIIA mean (S.D.)	*n*[c]
Class 1, reduced binding to all FcγR						
E233P	0.54 (0.20) 3	0.12 (0.06) 6	0.08 (0.01)	0.12 (0.01)	0.04 (0.02)	2
L234V						
L235A						
G236 deleted						
P238A	1.49 (0.17) 3	0.60 (0.05) 5	0.38 (0.14)	0.36 (0.15)	0.07 (0.05)	4
D265A	1.23 (0.14) 4	0.16 (0.05) 9	0.07 (0.01)	0.13 (0.05)	0.09 (0.06)	4
N297A	0.80 (0.18) 8	0.15 (0.06) 7	0.05 (0.00)	0.10 (0.02)	0.03 (0.01)	3
A327Q	0.97	0.60 (0.12) 9	0.13 (0.03)	0.14 (0.03)	0.06 (0.01)	4
P329A	0.80	0.48 (0.10) 6	0.08 (0.02)	0.12 (0.08)	0.21 (0.03)	4
Class 2, reduced binding to FcγRII and FcγRIIIA						
D270A	1.05	0.76 (0.12) 6	0.06 (0.02)	0.10 (0.06)	0.14 (0.04)	6
Q295A	0.79	1.00 (0.11) 4	0.62 (0.20)	0.50 (0.24)	0.25 (0.09)	5
A327S		0.86 (0.03) 4	0.23 (0.06)	0.22 (0.05)	0.06 (0.01)	4
Class 3, improved binding to FcγRII and FcγRIIIA						
T256A	1.91 (0.43) 6	1.01 (0.07) 5	1.41 (0.27)	2.06 (0.66)	1.32 (0.18)	9
K290A	0.79 (0.14) 3	1.01 (0.06) 11	1.30 (0.21)	1.38 (0.17)	1.31 (0.19)	9
Class 4, improved binding to FcγRII and no effect on FcγRIIIA						
R255A	0.59 (0.19) 4	0.99 (0.12) 7	1.30 (0.20)	1.59 (0.42)	0.98 (0.18)	5
E258A	1.18	1.18 (0.13) 4	1.33 (0.22)	1.65 (0.38)	1.12 (0.12)	5
S267A	1.08	1.09 (0.08) 10	1.52 (0.22)	1.84 (0.43)	1.05 (0.24)	11
E272A	1.34 (0.24) 4	1.05 (0.06) 7	1.23 (0.12)	1.53 (0.22)	0.80 (0.18)	6
N276A	1.15 (0.21) 3	1.05 (0.14) 4	1.29 (0.20)	1.34 (0.40)	0.95 (0.04)	4
D280A	0.82	1.04 (0.08) 10	1.34 (0.14)	1.60 (0.31)	1.09 (0.20)	10
H285A	0.85	0.96 (0.07) 4	1.26 (0.12)	1.23 (0.15)	0.87 (0.04)	4
N286A	1.24 (0.04) 2	0.95 (0.18) 16	1.24 (0.23)	1.36 (0.15)	1.05 (0.04)	6
T307A	1.81 (0.32) 6	0.99 (0.14) 4	1.07 (0.15)	1.27 (0.24)	1.09 (0.18)	10
L309A	0.63 (0.18) 4	0.93 (0.18) 6	1.13 (0.08)	1.26 (0.12)	1.07 (0.20)	3
N315A	0.76 (0.14) 3	0.99 (0.16) 6	1.15 (0.06)	1.30 (0.17)	1.07 (0.21)	5
K326A	1.03	1.03 (0.05) 10	1.23 (0.20)	1.41 (0.27)	1.23 (0.23)	7
P331A	0.85	1.01 (0.09) 7	1.29 (0.14)	1.34 (0.35)	1.08 (0.19)	4
S337A	1.03	1.17 (0.23) 3	1.22 (0.30)	1.26 (0.06)	0.94 (0.18)	4
A378Q	1.32 (0.13) 3	1.06 (0.05) 3	1.40 (0.17)	1.45 (0.17)	1.19 (0.17)	5
E430A	0.93 (0.03) 2	1.05 (0.02) 3	1.24 (0.11)	1.28 (0.10)	1.20 (0.18)	5
Class 5, improved binding to FcγRII and reduced binding to FcγRIIIA						
H268A	1.02 (0.22) 3	1.09 (0.11) 8	1.21 (0.14)	1.44 (0.22)	0.54 (0.12)	13
R301A	0.86	1.06 (0.10) 4	1.14 (0.13)	1.29 (0.16)	0.22 (0.08)	7
K322A	0.98	0.94 (0.04) 9	1.17 (0.11)	1.28 (0.21)	0.62 (0.12)	6
Class 6, reduced binding to FcγRII and no effect on FcγRIIIA						
R292A	0.81 (0.18) 4	0.95 (0.05) 8	0.27 (0.13)	0.17 (0.07)	0.89 (0.17)	10
K414A	1.02	1.00 (0.04) 3	0.64 (0.15)	0.58 (0.18)	0.82 (0.27)	3
Class 7, reduced binding to FcγRII and improved binding to FcγRIIIA						
S298A	0.80	1.11 (0.03) 9	0.40 (0.15)	0.23 (0.13)	1.34 (0.20)	16
Class 8, no effect on FcγRII and reduced binding to FcγRIIIA						
S239A	1.06	0.81 (0.09) 7	0.73 (0.25)	0.76 (0.36)	0.26 (0.08)	3
E269A	1.05	0.61 (0.14) 9	0.65 (0.18)	0.75 (0.29)	0.45 (0.13)	5
E293A	0.85	1.11 (0.07) 4	1.08 (0.19)	1.07 (0.20)	0.31 (0.13)	6
Y296F	0.79	1.03 (0.09) 8	0.97 (0.23)	0.86 (0.17)	0.55 (0.12)	6
V303A	1.26 (0.21) 3	0.91 (0.11) 5	0.86 (0.10)	0.65 (0.17)	0.33 (0.09)	8
A327G		0.96 (0.01) 3	0.92 (0.09)	0.83 (0.10)	0.36 (0.05)	3
K338A	1.14	0.90 (0.05) 3	0.78 (0.09)	0.63 (0.08)	0.15 (0.01)	2
D376A	1.45 (0.36) 4	1.00 (0.05) 3	0.80 (0.16)	0.68 (0.14)	0.55 (0.10)	5
Class 9, no effect on FcγRII and improved binding to FcγRIIIA						
E333A	1.03 (0.01) 2	0.98 (0.15) 5	0.92 (0.12)	0.76 (0.11)	1.27 (0.17)	10
K334A	1.05 (0.03) 2	1.06 (0.06) 11	1.01 (0.15)	0.90 (0.12)	1.39 (0.19)	16
A339T		1.06 (0.04) 6	1.09 (0.03)	1.20 (0.03)	1.34 (0.09)	2
Class 10, affect only FcRn						
I253A	<0.10	0.96 (0.05) 4	1.14 (0.02)	1.18 (0.06)	1.08 (0.14)	3
S254A	<0.10	0.96 (0.08) 4	0.97 (0.24)	1.15 (0.38)	0.73 (0.14)	3
K288A	0.38 (0.12) 5	0.88 (0.15) 15	1.15 (0.26)	1.14 (0.20)	1.06 (0.04)	4
V305A	1.46 (0.48) 6	1.04 (0.19) 10	1.12 (0.12)	1.23 (0.22)	0.84 (0.15)	4
Q311A	1.62 (0.25) 4	0.93 (0.05) 4	1.11 (0.06)	1.19 (0.13)	0.93 (0.17)	3
D312A	1.50 (0.06) 4	1.01 (0.12) 5	1.20 (0.24)	1.19 (0.07)	1.23 (0.14)	3
K317A	1.44 (0.18) 4	0.92 (0.17) 6	1.13 (0.05)	1.18 (0.27)	1.10 (0.23)	4
K360A	1.30 (0.08) 4	1.02 (0.04) 3	1.12 (0.10)	1.12 (0.08)	1.23 (0.16)	6
Q362A	1.25 (0.24) 3	1.00 (0.04) 3	1.03 (0.10)	1.02 (0.03)	1.03 (0.16)	4
E380A	2.19 (0.29) 6	1.04 (0.06) 3	1.18 (0.01)	1.07 (0.05)	0.92 (0.12)	2
E382A	1.51 (0.18) 4	1.06 (0.03) 3	0.95 (0.11)	0.84 (0.04)	0.76 (0.17)	3
S415A	0.44	1.04 (0.03) 3	0.90 (0.11)	0.88 (0.05)	0.86 (0.18)	2
S424A	1.41 (0.14) 3	0.98 (0.03) 3	1.04 (0.06)	1.02 (0.02)	0.88 (0.09)	2
H433A	0.41 (0.14) 2	0.98 (0.03) 3	0.92 (0.18)	0.79 (0.18)	1.02 (0.15)	3
N434A	3.46 (0.37) 7	1.00 (0.04) 3	0.96 (0.06)	0.97 (0.12)	0.77 (0.13)	6
H435A	<0.10 4	1.25 (0.09) 3	0.77 (0.05)	0.72 (0.05)	0.78 (0.03)	3
Y436A	<0.10 2	0.99 (0.02) 2	0.93 (0.05)	0.91 (0.06)	0.91 (0.15)	3

[a] Residue numbers are according to the Eu numbering system (18). Variants that had no effect on binding (*i.e.* did not reduce binding by more than 60% or improve binding by more than 20%) to FcγR or FcRn were as follows: Lys^{246}, Lys^{248}, Asp^{249}, Met^{252}, Thr^{260}, Lys^{274}, Tyr^{278}, Val^{282}, Glu^{283}, Thr^{289}, Glu^{294}, Y300F, Glu^{318}, Lys^{320}, Ser^{324}, A330Q, Thr^{335}, Lys^{340}, Gln^{342}, Arg^{344}, Glu^{345}, Gln^{347}, Arg^{355}, Glu^{356}, Met^{358}, Thr^{359}, Lys^{360}, Asn^{361}, Tyr^{373}, Ser^{375}, Ser^{383}, Asn^{384}, Gln^{386}, Glu^{388}, Asn^{389}, Asn^{390}, Y391F, Lys^{392}, Leu^{398}, Ser^{400}, Asp^{401}, Asp^{413}, Arg^{416}, Gln^{418}, Gln^{419}, Asn^{421}, Val^{422}, Thr^{437}, Gln^{438}, Lys^{439}, Ser^{440}, Ser^{442}, Ser^{444}, and Lys^{447}.

[b] Values are the ratio of binding of the variant to that of native IgG1 at 0.33 or 1 μg/ml. A value greater than 1 denotes binding of the variant was improved compared with native IgG1, whereas a ratio less than 1 denotes reduced binding compared with native IgG1. Reduced binding to any given receptor was defined as a reduction of ≥40% compared to native IgG; better binding was defined as an improvement of ≥25% compared with native IgG1.

[c] Number of independent assays for FcγRIIA, FcγRIIB and FcγRIIIA. At least two separately expressed and purified lots of each variant were assayed.

The Journal of Biological Chemistry jbc

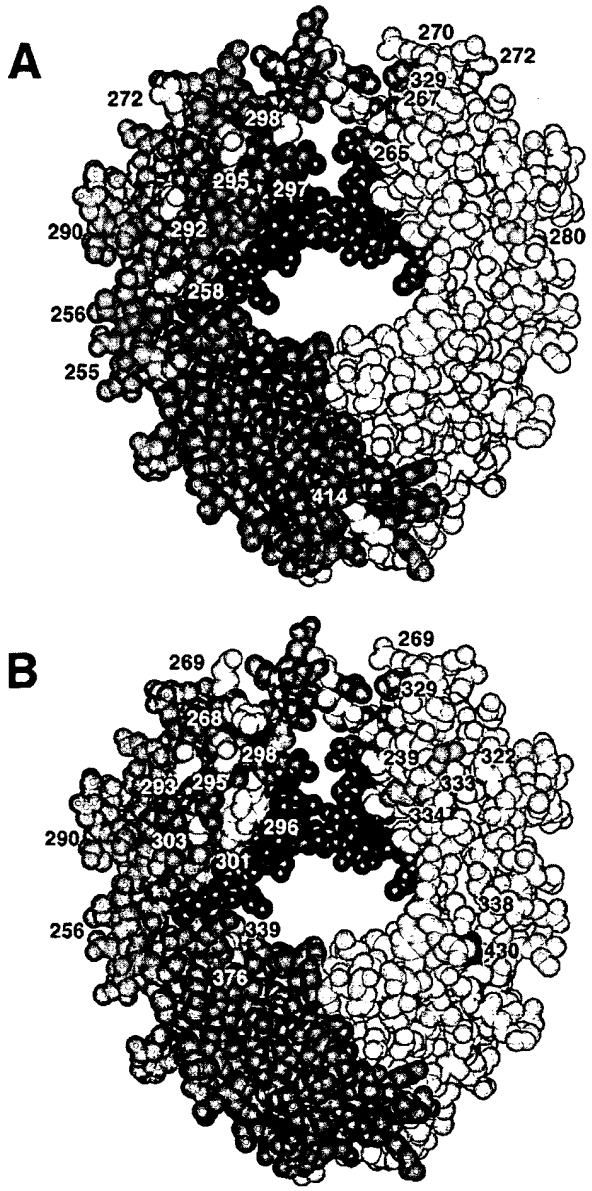

FIG. 2. **Binding sites of human IgG1 for FcγR.** *A*, IgG1 residues comprising the binding site for FcγRI and FcγRII. The two Fc heavy chains are in *light* and *medium gray*; carbohydrate is in *dark gray*. Residues that affected binding to all FcγR are in *red*; the FcγRI binding site is composed only of *red* residues. Residues that showed improved binding to FcγRII and FcγRIIIA are in *magenta*. Residues that showed reduced binding only to FcγRII are in *yellow*. Residues that showed ≥ 50% improved binding only to FcγRII are in *green*. *B*, IgG1 residues comprising the binding site for FcγRI and FcγRIIIA. The two Fc heavy chains are in *light* and *medium gray*; carbohydrate is in *dark gray*. Residues that affected binding to all FcγR are in *red*; the FcγRI binding site is composed only of *red* residues. Residues that showed improved binding to FcγRII and FcγRIIIA are in *magenta*. Residues that showed reduced binding only to FcγRIIIA are in *yellow*. Residues that showed ≥ 25% improved binding only to FcγRIIIA are in *green*. Glu^{430}, involved in a salt-bridge with Lys^{338}, is shown in *blue*.

Class 2 consists of three variants with reduced binding to FcγRII and FcγRIII but not FcγRI. Like the residues in Class 1, Asp^{270} and Gln^{295} are located near the hinge (Fig. 2*A*). In crystal structures of human IgG1 Fc (30, 59), Gln^{295} is completely solvent-exposed, whereas Asp^{270}, although exposed, forms hydrogen bonds from its side chain O-δ atom to the backbone nitrogens of Lys^{326} and Ala^{327} and to the side chain N-δ of Asn^{325}. Disruption of these interactions by D270A could cause a local conformational perturbation that affected the severe reduction in binding to FcγRII and FcγRIIIA. However, D270A did not affect binding to FcγRI or FcRn. Furthermore, D270N, which could maintain the aforementioned hydrogen bonds, also abolished binding to FcγRII and FcγRIIIA, and D270E bound to FcγRIIIA as effectively as did native IgG1 (Table II). Taken together, these data suggest that the side chain charge of Asp^{270} is important for interaction with FcγRII and FcγRIIIA.

Class 3 consists of two variants with improved binding to FcγRIIA, FcγRIIB, and FcγRIIIA. Thr^{256} and Lys^{290} are located near one another in the CH2 domain (Fig. 2). T256A also exhibited improved binding to FcRn; indeed altering Thr^{256} in murine IgG1 to other residues improved binding to murine FcRn (13).

Class 4 variants were characterized by improved binding only to FcγRIIA and FcγRIIB. Those that improved binding to FcγRII the most, R255A, E258A, S267A, E272A, and D280A, are distant from one another in the CH2 domain (Fig. 2*A*). Of these, only Ser^{267} was cited as an interacting residue in the Fc:FcγRIIA crystal structure (26). S267A improved binding only to FcγRII, S267G abolished binding only to FcγRIIIA, and S267T reduced binding to FcγRII and FcγRIIIA (Tables I and II). D280N (Table II), like D280A (Table I), improved binding only to FcγRII. Three of the Class 4 residues also exhibited improved binding to FcRn (E272A, T307A, and A378Q), whereas R255A exhibited reduced binding. Ala^{378} interacts with CH2 domain loop AB, which contains residues that interact directly with FcRn, and hence may influence binding to FcRn indirectly.

Class 5 variants exhibited improved binding to FcγRIIA and FcγRIIB but, in contrast to Class 4, also showed reduced binding to FcγRIIIA. Of these, Lys^{322} has also been implicated in human C1q binding (55). The aliphatic portion of the Arg^{301} side chain is buried and interacts with the Tyr^{296} side chain, at least in some crystal structures, whereas the Arg^{301} guanidinium group may interact with the Asn^{297}-linked carbohydrate (30, 59, 60). The R301A variant effected a modest improvement in binding to FcγRIIB and a pronounced reduction in binding to FcγRIIIA (Table I); the R301M variant, which may maintain the aliphatic interaction of the Arg^{301} side chain, showed improved binding to FcγRIIA and FcγRIIB and a less pronounced reduction of binding to FcγRIIIA compared with R301A (Table II).

Class 6 residues show diminished binding to FcγRII only. R292A is located in the CH2 domain distant from the hinge. Lys^{414} is at the "bottom" of the IgG1, spatially removed from all other residues having an effect on FcγRII binding, suggesting that it may play only a minor role in binding (discussed below).

Class 7 is composed of S298A that reduced binding to FcγRII but improved binding to FcγRIIIA. Situated among the Class 1 residues near the hinge (Fig. 2), Ser^{298} is also part of the Asn-linked glycosylation sequence Asn^{297}–Ser^{298}–Thr^{299}. S298T followed the pattern of S298A, whereas S298N abolished binding to FcγRIIIA as well as FcγRII (Table II).

Reduced binding only to FcγRIIIA characterizes Class 8 and includes five residues in the CH2 domain and two in the CH3 domain (Ala^{327} is in Class 1). Ser^{239} has been previously identified as playing a minor role in murine IgG2b binding to murine FcγRII (25), and in the IgG1 Fc:FcγRIIIA crystal structure (26), the Ser^{239} in one of the two heavy chains forms a hydrogen bond to the Lys^{117} side chain of FcγRIIIA. In contrast, E293A (Table I) and E293D (Table II) reduced binding as much as did S239A even though Glu^{293} is not located near the Fc:FcγRIIIA interface in the crystal structure. In some crystal structures (30, 59, 60), the Tyr^{296} side chain interacts inti-

TABLE II
Binding of human IgG1 non-Ala variants to human FcγRII and FcγRIIIA

Variant[a]	FcγRIIA[b] mean (S.D.)	FcγRIIB mean (S.D.)	FcγRIIIA mean (S.D.)	n[c]
D265N	0.02 (0.01)	0.03 (0.01)	0.02 (0.01)	3
D265E	0.11 (0.04)	0.03 (0.01)	0.02 (0.01)	3
S267G	1.18 (0.10)	0.95 (0.14)	0.08 (0.02)	4
S267T	0.42 (0.10)	0.45 (0.01)	0.05 (0.05)	3
D270N	0.03 (0.02)	0.05 (0.05)	0.04 (0.03)	5
D270E	0.08 (0.01)	0.06 (0.01)	0.90 (0.17)	3
D280N	1.07 (0.18)	1.22 (0.19)	1.16 (0.21)	6
E293D	0.90 (0.02)	0.88 (0.07)	0.37 (0.07)	3
S298T	0.29 (0.19)	0.27 (0.19)	0.73 (0.21)	6
S298N	0.05 (0.03)	0.08 (0.08)	0.06 (0.03)	5
R301M	1.29 (0.17)	1.56 (0.12)	0.48 (0.21)	4
P331S	0.91 (0.08)	0.78 (0.07)	0.58 (0.19)	4
E333Q	0.70 (0.05)	0.64 (0.09)	1.05 (0.09)	3
E333N	0.59 (0.04)	0.52 (0.07)	0.56 (0.10)	4
E333D			1.26 (0.04)	3
K334R	1.15 (0.09)	1.33 (0.18)	0.68 (0.07)	5
K334Q	1.08 (0.11)	1.10 (0.21)	1.23 (0.08)	7
K334N	1.16 (0.11)	1.29 (0.30)	1.11 (0.12)	8
K334E	0.74 (0.15)	0.72 (0.12)	1.30 (0.09)	6
K334V	1.13 (0.11)	1.09 (0.15)	1.34 (0.18)	3
K338M	0.99 (0.13)	0.93 (0.15)	0.49 (0.04)	2

[a] Residue numbers are according to the Eu numbering system (18).
[b] Values are the ratio of binding of the variant to that of native IgG1 at 0.33 or 1 μg/ml. A value greater than 1 denotes binding of the variant was improved compared with native IgG1, whereas a ratio less than 1 denotes reduced binding compared to native IgG1.
[c] Number of independent assays for FcγRIIA, FcγRIIB, and FcγRIIIA. At least two separately expressed and purified lots of each variant were assayed.

mately with the aliphatic portion of Arg^{301} (Class 5); altering either of these reduced binding to FcγRIIIA. Note, however, that Tyr^{296} was changed to Phe (not Ala) and the 50% reduction in binding to FcγRIIIA was due only to removal of the side chain hydroxyl group.

At position Lys^{338}, altering the side chain to Ala or Met affected reduction in binding to FcγRIIIA, suggesting that both the side chain charge and aliphatic portions are required. The Lys^{338} side chain forms part of the interface between the CH2 and CH3 domains and participates in a salt bridge with Glu^{430} in several crystal structures (30, 60, 61) (Fig. 2*B*). Although it is possible that altering Lys^{338} may disrupt the CH2:CH3 interface and thereby influence binding, K338A (Table I) and K338M (Table II) did not disrupt binding to FcγRI, FcγRII, or FcRn. Since it is known that binding of IgG1 to FcRn involves residues in both CH2 and CH3 (27–29), this suggests that any conformational effect of K338A must be local and minimal. Note also that while K338A and K338M reduced binding to FcγRIIIA, E430A (Class 4) improved binding, suggesting that the Lys^{338}:Glu^{430} salt bridge is not essential in maintaining binding. Another CH3 residue affecting FcγRIIIA is Asp^{376} that interacts with the CH2 domain.

Class 9 is characterized by improved binding only to FcγRIIIA and includes E333A, K334A, and A339T. A previous study found that A339T improved binding to FcγRI (62); in this study the A339T variant bound better than native IgG1 to FcγRIIIA but not FcγRI (Table I). Several non-Ala variants were tested at Glu^{333} and Lys^{334}. E333D also improved binding to FcγRIIIA, whereas E333N reduced binding to FcγRII as well as FcγRIIIA (Table II). At position 334, changing Lys to Gln, Glu, or Val maintained the improved binding to FcγRIIIA (Table II). Surprisingly, the K334R variant reversed the receptor preference, *i.e.* this variant bound better to FcγRIIB and not FcγRIIIA as for the K334A variant. Taken together these data suggest that FcγRIIIA interacts with Lys^{334} even though this residue is not among the IgG1 residues found to interact with FcγRIIIA in the co-crystal structure (26).

Class 10 residues influenced binding only to FcRn. Note that residues in other classes may also have affected binding to FcRn but were classified according to their effect on FcγR. Positions that effectively abrogated binding to FcRn when changed to alanine include Ile^{253}, Ser^{254}, His^{435}, and Tyr^{436}. Other positions showed a less pronounced reduction in binding as follows: Glu^{233}–Gly^{236} (Class 1), Arg^{255} (Class 4), Lys^{288}, Ser^{415}, and His^{433}. Several amino acid positions exhibited an improvement in FcRn binding when changed to alanine; notable among these are Pro^{238} (Class 1), Thr^{256} (Class 3), Thr^{307} (Class 4), Gln^{311}, Asp^{312}, Glu^{380}, Glu^{382}, and Asn^{434}. The pattern of binding was the same when a second assay format was used, *e.g.* with IgE-coated plates rather than FcRn-coated plates.

Binding of Combination Variants—A number of combination variants were tested in which two or more residues were simultaneously altered to Ala. Some of these combinations showed additive effects. An example is the E258A/S267A variant that exhibited binding to FcγRIIA, and FcγRIIB that was better than the E258A (Class 4) and S267A (Class 4) variants (Tables I and III). A similar outcome was found for the S298A/E333A and S298A/K334A variants in which the binding to FcγRIIIA improved over the parental variants (Table III). In other combinations, one residue dominated the other, *e.g.* the T256A/S298A variant showed reduced binding to FcγRIIA and FcγRIIB similar to the S298A variant even though the T256A change effected better binding to both these receptors (Class 3).

The most pronounced additivity was found for combination variants with improved binding to FcRn. At pH 6.0, the E380A/N343A variant showed over 8-fold better binding to FcRn, relative to native IgG1, compared with 2-fold for E380A and 3.5-fold for N434A (Tables I and III). Adding T307A to this effected a 13-fold improvement in binding relative to native IgG1. Likewise, combining E380A and L309A, the latter being deleterious to FcRn binding, resulted in a variant that was intermediate between the two parental variants (Table III). As with the FcγR, some combinations showed dominance of one residue over the other; for the K288A/N434A variant, the better binding due to N434A clearly overcame the reduction in binding from K288A (Table III). As expected from previous studies (28), at pH 7.2 none of variants bound well (data not shown).

Role of IgG Residues Affecting Carbohydrate—Previously it

TABLE III
Binding of human IgG1 combination variants to human FcRn and FcγR

Variant[a]	FcRn[b] mean (S.D.) *n*	FcγRIIA[c] mean (S.D.) *n*	FcγRIIB mean (S.D.) *n*	FcγRIIIA mean (S.D.) *n*
S267A H268A		1.41 (0.00) 2	1.56 (0.16) 2	0.96 (0.12) 2
S267A E258A		1.62 (0.15) 2	2.01 (0.45) 2	1.04 (0.12) 2
S267A R255A		1.60 (0.18) 3	1.72 (0.13) 3	0.88 (0.07) 3
S267A E272A		1.51 (0.13) 3	1.82 (0.32) 3	0.95 (0.05) 3
T256A S298A		0.44 (0.03) 2	0.22 (0.04) 2	1.41 (0.06) 2
S298A E333A		0.34 (0.05) 5	0.16 (0.08) 5	1.53 (0.24) 5
S298A K334A		0.41 (0.07) 6	0.19 (0.08) 6	1.62 (0.34) 6
S298A E333A K334A		0.34 (0.15) 10	0.15 (0.06) 10	1.51 (0.31) 10
E380A N434A	8.0 (1.0) 6	1.02 (0.07) 2	1.05 (0.11) 2	1.02 1
T307A E380A N434A	11.8 (1.5) 5	0.99 (0.06) 2	0.99 (0.11) 2	0.96 1
L309A E380A	0.9 (0.1) 4	0.98 1	1.04 1	0.92 1
K288A N434A	2.9 (0.4) 4	0.94 (0.11) 2	0.96 (0.17) 2	0.88 1

[a] Residue numbers are according to the Eu numbering system (18).
[b] Values are the ratio of binding of the variant to that of native IgG1 at pH 6.0.
[c] Values are the ratio of binding of the variant to that of native IgG1 at 0.33 or 1 μg/ml. A value greater than 1 denotes binding of the variant was improved compared with native IgG1, whereas a ratio less than 1 denotes reduced binding compared with native IgG1.

was noted that replacing human IgG3 residues that contact the oligosaccharide, *e.g.* Asp^{265}, Tyr^{296}, and Arg^{301}, with Ala resulted in increased galactosylation and sialylation relative to native IgG3 and in reduced binding to both FcγR and C1q (56). To determine if the effect seen for specific Ala substitutions (either deleterious or advantageous) was due to differences in glycosylation, oligosaccharide analysis was performed for selected variants (Table IV). The D265A, R301A, and R301M variants showed increased galactosylation, a relatively small amount of sialylation, and a small percentage of triantennary carbohydrate, in agreement with Lund *et al.* (56). The R301A and R301M variants also showed an increase in fucose and a decrease in mannose not seen previously. For the Y296F variant, there were no differences from native IgG1, in contrast to the decrease in galactose and fucose and increase in mannose reported by Lund *et al.* (56). These differences may be due to the different mammalian cells used to express the antibodies (human kidney 293 cells in this study and Chinese hamster ovary cells in the previous study) or may reflect that Tyr^{296} was changed to Phe^{296} in this study, whereas it was changed to Ala^{296} in the Lund *et al.* (56) study.

The Lys^{334} side chain is near the carbohydrate in IgG crystal structures but does not interact with it as intimately as do Asp^{265}, Tyr^{296}, and Arg^{301}. The K334A variant exhibited a small increase in mannose and small decrease in fucose compared with native IgG1 (Table IV). Ser^{298} interacts with the carbohydrate only through its O-γ atom, which forms a hydrogen bond to the Asn^{297} O-δ, and no difference in carbohydrate for the S298A was evident compared with native IgG1. Neither the Glu^{258} or Val^{303} side chains interact with the carbohydrate, and indeed both are located on the opposite face of the CH2 domain from the carbohydrate. However, the E258A variant showed an increase in galactosylation and a small amount of sialic acid, whereas the V303A variant only showed a small amount of sialic acid. Hence, variation in galactosylation and sialic acid for a given variant (compared with native IgG1) may occur regardless of whether the amino acid side chain interacts with the carbohydrate.

For the Y296F, S298A, V303A, and K334A variants, the differences in glycosylation, compared with native IgG1, were minimal and most likely were not the cause of the differences in binding of these variants to the FcγR. For the E258A, D265A, R301A, and R301M variants, it is difficult to discern whether reduction or improvement in FcγR binding is due to the change in amino acid side chain or from differences in glycosylation.

Binding to Allotypic Forms of FcγRIIA and FcγRIIIA—Selected variants were tested for binding to the FcγRIIA-His^{131} and FcγRIIIA-Val^{158} allotypic receptor forms based on their improved or reduced binding to the allotypic forms used for the assays (*i.e.* FcγRIIA-Arg^{131} and FcγRIIIA-Phe^{158}). Table V shows that most of the variants bound equivalently to the FcγRIIA-Arg^{131} and FcγRIIA-His^{131} receptors. The exceptions were the S267A, H268A, and S267A/H268A variants that displayed binding to FcγRIIA-His^{131} that was reduced compared with FcγRIIA-Arg^{131} but still equivalent to native IgG1. The related S267G variant, however, showed a 50% reduction in binding to the FcγRIIA-His^{131} receptor compared with native IgG1. In contrast to S267A and H268A, D270A reduced binding to FcγRIIA-His^{131} by 50% but completely abrogated binding to FcγRIIA-Arg^{131}. This suggests that Ser^{267}, His^{268}, and Asp^{270} interact with FcγRIIA in the vicinity of FcγRIIA residue 131.

For FcγRIIIA, the selected variants were assayed in the ELISA format as well as on stable-transfected CHO cell lines expressing the α-chains (FcγRIIIA-Phe^{158} or FcγRIIIA-Val^{158}) with the associated human γ-chain. For FcγRIIIA-Phe^{158}, those variants that showed improved binding in the ELISA format

TABLE IV
Percent of total oligosaccharide area by glycan type

	IgG1	E258A	D265A	Y296F	S298A	R301A	R301A	V303M	K334A
High mannose									
	14.6[a]	11.1	8.0	14.8	11.3	5.3	5.4	10.2	20.9
	3.8	1.1	4.0			0.8	2.4	0.7	
Complexes with terminal galactose									
0	51.5	36.3	47.2	47.0	48.9	24.1	24.3	48.7	49.5
	0.6	0.2	6.0			3.7	0.9	0.2	
1	23.4	34.9	25.0	23.1	28.1	23.9	27.2	28.5	17.4
	3.2	0.9	3.5			0.8	5.9	0.5	
2	8.5	15.8	19.5	12.5	9.6	45.3	42.0	11.4	10.8
	0.3	0.1	6.3			2.4	5.9	0.4	
3	2.0	2.0	0.2	2.5	2.1	1.1	1.1	1.0	1.5
	0.5	0.2	0.2			1.0	0.3	0.1	
1–3	33.9	52.7	44.7	38.1	39.8	70.3	70.3	40.9	29.7
	4.0	1.2	10.0			4.0	1.7	1.0	
Complexes with terminal sialic acid									
	0.0	3.0	2.4	0.0	0.0	9.7	10.9	1.3	0.0
Complexes with fucose									
0	4.5	1.1	1.3	3.0	1.5	0.7	1.5	1.6	6.1
	0.6	0.1	0.2			0.2	1.9	0.2	
1	81.1	87.9	90.7	82.1	87.2	94.0	93.4	88.1	73.1
	3.0	1.3	3.9			1.0	1.5	0.5	
Triantennary complexes									
	0.2	0.2	3.2	0.0	0.0	5.5	5.0	0.3	0.0
	0.2	0.2	0.1			1.2	0.8	0.3	

[a] Upper values are mean percent and lower values are deviation from mean for two independent analyses on two different lots of IgG.

TABLE V
Binding of human IgG1 variants to human FcγRIIA-R131 and FcγRIIA-H131 polymorphic receptors

Variant[a]	Class[b]	FcγR (S.D.)	FcγRIIA-Arg^{131}[c] mean (S.D.) *n*	FcγRIIA-Arg^{131}[d] mean (S.D.)	FcγRIIA-His^{131} mean (S.D.)	His^{131}/Arg^{131} mean (S.D.)	*n*[e]
S267A	4	↑ ||	1.52 (0.22) 11	1.53 (0.06)	1.10 (0.12)	0.71 (0.07)	5
S267G		↓ |||	1.18 (0.10) 4		0.54 (0.14)	0.47 (0.13)	5
H268A	5	↑ || ↓ |||	1.21 (0.14) 13	1.30 (0.17)	0.97 (0.15)	0.75 (0.12)	10
D270A	2	↓ ||,|||	0.06 (0.01) 5	0.04 (0.02)	0.45 (0.11)	16.6 (8.5)	6
S298A	7	↓ || ↑ |||	0.40 (0.15) 16	0.26 (0.10)	0.24 (0.08)	0.93 (0.13)	6
V305A	10	↑ FcRn	1.12 (0.12) 4	1.00 (0.14)	1.06 (0.10)	1.08 (0.10)	4
T307A	4	↑ ||	1.07 (0.14) 11	1.28 (0.13)	1.18 (0.06)	0.94 (0.09)	5
N315A	4	↑ ||	1.15 (0.06) 5	1.11 (0.18)	1.10 (0.16)	0.99 (0.05)	8
K317A	10	↑ FcRn	1.13 (0.05) 4	1.10 (0.13)	1.08 (0.08)	0.99 (0.07)	7
K320A		No effect	1.14 (0.11) 6	1.05 (0.19)	1.13 (0.09)	1.10 (0.15)	7
S267A H268A		↑ ||	1.41 (0.00) 2	1.57 (0.06)	1.02 (0.08)	0.65 (0.03)	4

[a] Residue numbers are according to the Eu numbering system (18).
[b] Class as noted in Table I.
[c] Values are from Tables I–III.
[d] Values are the ratio of binding of the variant to that of native IgG1 in assays separate from those in column 4 and performed simultaneously with the FcγRIIA-H131 assays in column 6.

exhibited even more improvement, compared with native IgG1, in the cell-based assay (Table VI). This could be due to the presence of the γ-chain associated with the α-chain enhancing binding of the IgG to FcγRIIIA (63). Alternatively, since the cell-based assay utilized monomeric IgG (in contrast to hexameric complexes used in the ELISA format assay), the cell-based assay may be less subject to an avidity component and thus more sensitive to changes in the binding interface. In contrast, none of the variants exhibited improved binding to the FcγRIIIA-Val^{158} receptor in the ELISA format assay, although the S298A, K334A, and S298A/E333A/K334A variants did bind better than native IgG1 in the cell-based assay.

ADCC Assays—ADCC assays were performed using a select set of variants to determine whether the improvement or reduction in binding seen in the ELISA format and cell-based assays were reiterated in a functional assay. For the ADCC assays, the IgG1 variants were generated in the Herceptin® (44) background since ADCC assays were not possible using the anti-IgE antibody. Chromium-57, calcein, and lactate dehydrogenase detection formats were used with either PBMCs or NKs, and the results were similar for all formats.

One set of ADCC assays with PBMCs compared the effect of D265A (Class 1), R292A (Class 6), and S298A (Class 7). The assay was repeated using four different donors. Fig. 3 shows that the ADCC pattern of the variants reiterated that seen in the ELISA binding assay for FcγRIIIA; D265A prevented ADCC ($p < 0.01$; paired t test); R292A had no effect, and S298A statistically improved ADCC ($p < 0.01$; paired t test).

A second set of assays was performed in which the FcγRIIIA allotype of the donors was determined. By using three FcγRIIIA-Val^{158}/Val^{158} and three FcγRIIIA-Phe^{158}/Phe^{158} donors, ADCC assays using only NK cells were repeated 3–4 times for each donor. Representative ADCC plots are shown in Fig. 4, *A* and *B*, and the summary of all assays is shown in Fig. 4*C*. The variants tested were as follows: S298A (Class 7), K334A (Class 9), S298A/K334A (Table III), and S298A/E333A/K334A (Table III). In agreement with the binding exhibited in the ELISA format assay (Tables I, III, and VI), the pattern of improved ADCC was S298A/E333A/K334A > S298A/K334A > S298A = K334A. This pattern was seen with both the

TABLE VI
Binding of human IgG1 variants to human FcγRIIIA-Phe[158] and FcγRIIIA-Val[158] polymorphic receptors

Variant[a]	Class[b]	FcγR	Phe[158c] mean (S.D.) *n*	Phe[158d] mean (S.D.)	Val[158e] mean (S.D.)	*n*[f]
D265A	1	↓ I,II,III	0.09 (0.06) 4	0.05 (0.02)	0.02 (0.01)	5
				0.12 (0.08)	0.05 (0.02)	3
K290A	3	↑ II,III	1.31 (0.19) 9	1.15 (0.27)	1.01 (0.08)	4
				1.61 (0.15)	0.89 (0.04)	3
S298A	7	↓ II ↑ III	1.34 (0.20) 16	1.49 (0.27)	1.07 (0.07)	7
				1.85 (0.05)	1.18 (0.09)	3
P331A	4	↑ II	1.08 (0.19) 3	1.00 (0.23)	0.97 (0.02)	5
				0.94 (0.07)	0.88 (0.09)	3
E333A	9	↓ II ↑ III	1.27 (0.17) 10	1.13 (0.32)	1.06 (0.11)	4
				1.42 (0.04)	1.08 (0.09)	3
K334A	9	↑ III	1.39 (0.19) 17	1.39 (0.22)	1.10 (0.07)	9
				2.46 (0.08)	1.26 (0.21)	3
S298A		↓ II ↑ III	1.51 (0.31) 10	2.17 (0.36)	1.11 (0.08)	5
E333A				3.42 (0.28)	1.65 (0.12)	3
K334A						

[a] Residue numbers are according to the Eu numbering system (18).
[b] Class as noted in Table I.
[c] Values are for FcγRIIIA-Phe[158] from Table I.
[d] Values are the ratio of binding of the variant to that of native IgG1 to FcγRIIIA-Phe[158] in assays separate from those in column 4 and performed simultaneously with the FcγRIIIA-Val[158] assays in column 6. Upper values are for binding in the ELISA format assay; lower values are for binding to CHO cells stable transfected with the α- and γ-chains of the receptor.
[e] Values are the ratio of binding of the variant to that of native IgG1 to FcγRIIIA-Val[158]. Upper values are for binding in the ELISA format assay; lower values are for binding to CHO cells stable transfected with the α- and γ-chains of the receptor.
[f] Number of independent assays for values in columns 5 and 6.

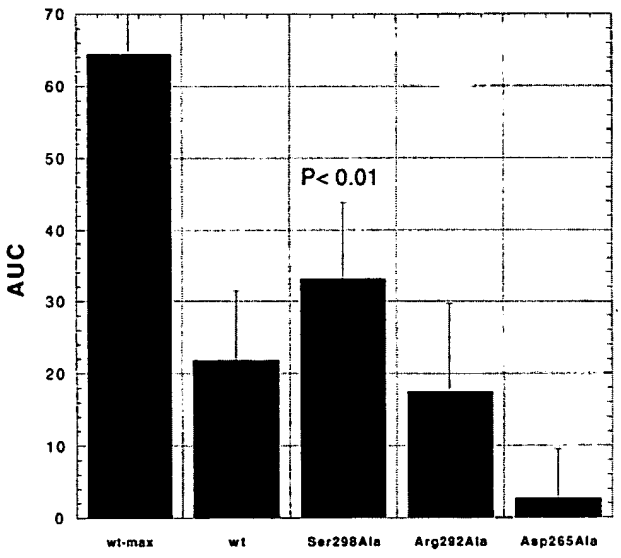

FIG. 3. **Antibody-dependent cell cytotoxicity of anti-p[185]HER2 IgG1 variants.** ADCC was performed using p[185]HER2-expressing SK-BR-3 cells as target. In four separate experiments, PBMCs isolated from four donors were used as effector cells. Cytotoxicity was detected by LDH release. SR of target cells and effector cells was measured using the respective cells alone; MR was measured by adding 2% Triton X-100 to target cells. AICC was measured using target and effector cells together (*i.e.* no antibody). Percent cytotoxicity was calculated as $((\text{LDH release}_{\text{sample}} - \text{SR}_{\text{effector}} - \text{SR}_{\text{target}})/(\text{MR}_{\text{target}} - \text{SR}_{\text{target}})) \times 100$. The log(effector/target ratio) was plotted *versus* percent cytotoxicity. The area *below* the curve (*AUC*) was calculated for each sample; AUC of AICC was subtracted from each sample, and the results were graphed in a bar plot for maximum cytotoxicity using 1 μg/ml anti-p[185]HER2 (*wt-max*), 2 ng/ml anti-p[185]HER2 (*wt*), 2 ng/ml S298A variant (Class 7), 2 ng/ml R292A (Class 6), and 2 ng/ml D265A (Class 1). $p < 0.01$ (paired *t* test) for S298A *versus* wt.

FcγRIIIA-Phe[158]/Phe[158] and FcγRIIIA-Val[158]/Val[158] donors, although improvement in ADCC was less pronounced for the latter. Comparing the improvement in binding to receptor for these variants in the ELISA format assay (Tables I, III, and VI) with that in the cell-based (Table VI) and ADCC assays (Figs. 3 and 4) shows that the improvement in binding for any specific variant is enhanced when the receptor is expressed on cells.

DISCUSSION

The Set of Human IgG1 Residues Involved in Binding to All Human FcγR—The set of IgG1 residues involved in binding to all human FcγR is represented by Class 1 (Table I). Indeed, this set comprises the entire binding site on IgG1 for FcγRI. Class 1 residues are located in the CH2 domain proximal to the hinge and fall into two categories as follows: 1) positions that may interact directly with all FcγR include Leu[234]–Pro[238], Ala[327], and Pro[329] (and possibly Asp[265]); 2) positions that influence carbohydrate nature or position include Asp[265] and Asn[297].

Previous studies mapping the binding residues in mouse or human IgG have concentrated primarily on the lower hinge region, *i.e.* residues Leu[234]–Ser[239], revealing Leu[234] and Leu[235] as the two most important for FcγRI (8, 19) and Leu[234] and Gly[237] as the two most important for FcγRII (25, 56). Of the two residues in the lower hinge investigated in this study, P238A affected binding to all FcγR, whereas S239A affected binding only to FcγRIIIA.

In the co-crystal structure of IgG1 Fc:FcγRIIIA (26), Pro[329] interacts with two Trp side chains from the receptor, and a similar interaction may occur with the other FcγR. However, removal of the Pro side chain, as in P329A, might cause a localized conformational change that perturbs adjacent binding residues, supported by the report that P329A also affects C1q binding (55). A327Q could be causing steric hindrance to binding due to introduction of a large side chain at this position, although altering Ala[327] to Ser did not affect binding to FcγRI. Inspection of the IgG1 Fc:FcγRIIIA crystal structure shows that Ala[327] is near the IgG1:FcγRIIIA interface and forms a van der Waals' interaction with the Trp[87] side chain; however, it is not obvious why introduction of a larger side chain such as Ser or Gln should so severely reduce binding. For Asn[297] and Asp[265], earlier studies evaluated the requirement for carbohydrate attached at Asn[297] as well as the influence of Asp[265] on the nature of the carbohydrate (12, 56, 57); these will be discussed below.

Human IgG1 Binding to FcγRI—For FcγRI the IgG segment Gly[316]–Ala[339] has also been previously implicated based on sequence comparison and binding of IgG subclasses from different species (21, 64) and mutagenesis (19, 62). Within the segment Gly[316]–Ala[339], however, only A327Q and P329A af-

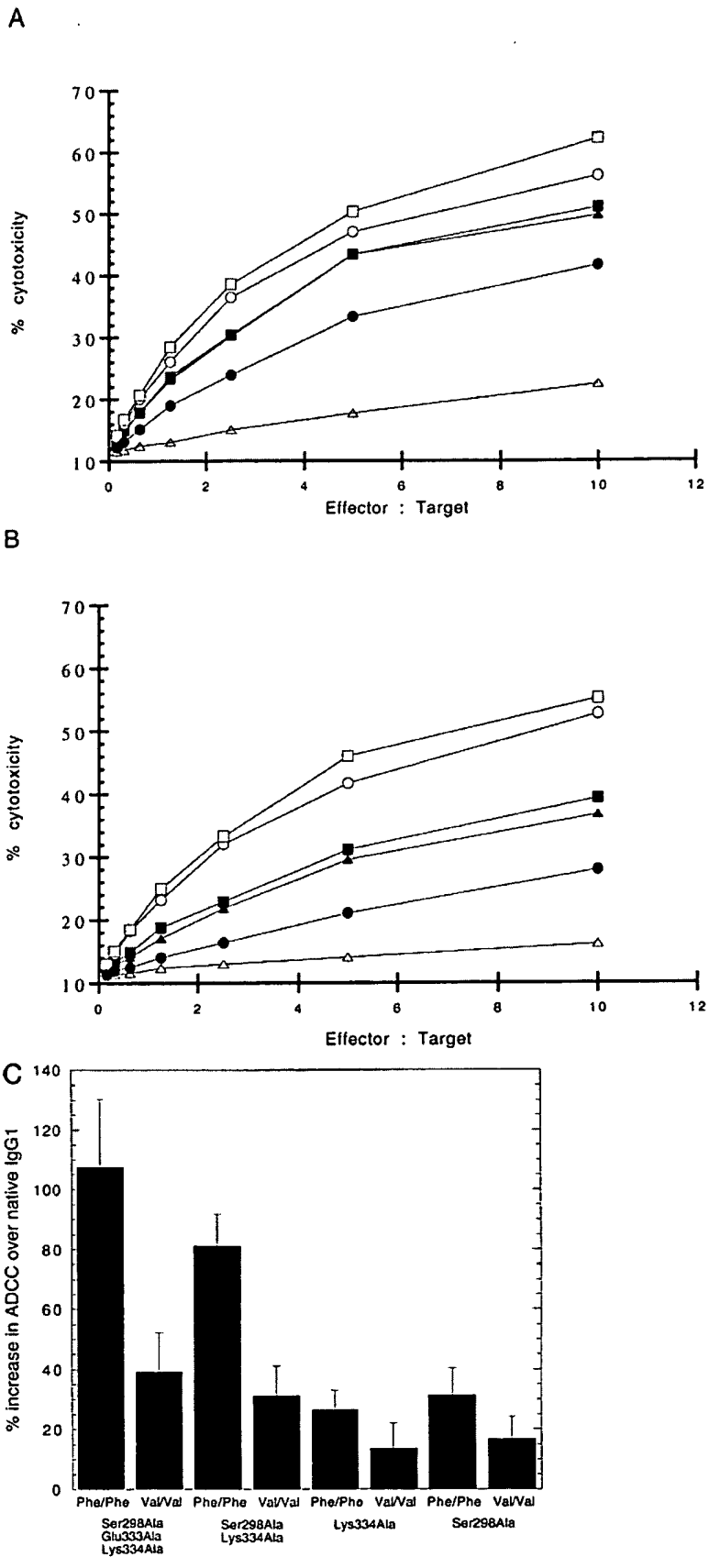

FIG. 4. **Antibody-dependent cell cytotoxicity of anti-p^{185}HER2 IgG1 variants for FcγRIIIA-Phe^{158} and FcγRIIIA-Val^{158} allotypes.** ADCC was performed using p^{185}HER2-expressing SK-BR-3 cells as target, and NKs isolated from three FcγRIIIA-Val^{158}/Val^{158} donors or three FcγRIIIA-Phe^{158}/Phe^{158} donors were used as effector cells. Cytotoxicity was detected by LDH release. AICC was measured using target and effector cells together (*i.e.* no antibody). MR was measured by adding 1% Triton X-100 to target cells. Percent cytotoxicity was calculated as (LDH release$_{sample}$/MR$_{target}$) × 100. The, effector/target ratio was plotted *versus* percent cytotoxicity. *A*, representative ADCC assay for IgG1 variants using NK cells from an FcγRIIIA-Val^{158}/Val^{158} donor. Native anti-p^{185}HER2 IgG1 (*solid circles*), S298A (*solid squares*), K334A (*solid triangles*), S298A/K334A (*open circles*), S298A/E333A/K334A (*open squares*), AICC (*open triangles*). *B*, representative ADCC assay for IgG1 variants using NK cells from an FcγRIIIA-Phe^{158}/Phe^{158} donor. Native anti-p^{185}HER2 IgG1 (*solid circles*), S298A (*solid squares*), K334A (*solid triangles*), S298A/K334A (*open circles*), S298A/E333A/K334A (*open squares*), AICC (*open triangles*). *C*, bar plot of mean percent increase in ADCC of variants compared with native anti-p^{185}HER2 IgG1. Percent increase was calculated as (% cytotoxicity$_{variant}$ − % cytotoxicity$_{native\ IgG1}$)/% cytotoxicity$_{native\ IgG1}$). For each variant, the mean and S.D. are for 13 data points using three different donors. For all variants the FcγRIIIA-Phe^{158}/Phe^{158} donors showed a significant increase in ADCC over the increase seen for FcγRIIIA-Val^{158}/Val^{158} donors ($p < 0.0001$ for all variants using paired *t* test).

fected binding to FcγRI (Class 1). All other exposed residues in the 316–339 segment had no effect. In contrast to a previous study in which changing residue 331 from Pro to Ser in human IgG3 reduced binding by 10-fold (19), in human IgG1 the P331A (Table I) and P331S (Table II) variants had no effect. Another previous report showed that an A339T substitution could improve binding to FcγRI by 3-fold (62); in this study the A339T variant was only equivalent in binding to native IgG1 (Class 3).

It has been noted that the presence of the γ-chain may augment the binding affinity of the FcγRI α-chain (63). Since it is conceivable that some residues in the human IgG1 might interact directly with the γ-chain, binding of the IgG1 variants to FcγRI on THP-1 cells was tested as well to the FcγRI α-chain coated on a plate. The results of the two assay formats were the same for the entire panel of variants, suggesting that the γ-chain augments binding by the α-chain through a mechanism other than direct interaction with the IgG1.

Since FcγRI binds monomeric IgG1 about 100-fold more strongly than do FcγRII and FcγRIII, one might expect that FcγRI would utilize either different or additional IgG1 residues to effect the tighter binding. However, the set of IgG1 residues that control binding to FcγRI are a subset of those effecting binding to FcγRII and FcγRIII (Class 1). This suggests that the comparatively strong binding of IgG1 to FcγRI results from either 1) utilization of only two Ig-like domains of FcγRI (analogous to the two Ig-like domains of FcγRII and FcγRIII) but with interaction of different amino acids on FcγRI than are used by FcγRII and FcγRIII, and 2) utilization of the same amino acids on all three receptors but with additional direct interaction of amino acids in the third FcγRI domain, or 3) the third domain of FcγRI effects a conformational change in the other two Ig-like domains that result in more efficacious interaction of these domains with the common set of binding residues on IgG1. In both human and murine FcγRI, removal of the third domain reduces affinity for monomeric IgG and alters specificity for IgG subclasses (65, 66). This would support, but does not discriminate between, possibilities 2 and 3.

Human IgG1 Binding to Human FcγRIIA and Human FcγRIIB—In contrast to FcγRI, FcγRII requires the presence of two identical IgG heavy chains (67), suggesting that residues from both heavy chains may form the FcγRII-binding site in IgG. The set of IgG1 residues, in addition to the common Class 1 residues, that affect binding to FcγRII are as follows: (largest effect) Arg^{255}, Thr^{256}, Glu^{258}, Ser^{267}, Asp^{270}, Glu^{272}, Asp^{280}, Arg^{292}, Ser^{298}, and (less effect) His^{268}, Asn^{276}, His^{285}, Asn^{286}, Lys^{290}, Gln^{295}, Arg^{301}, Thr^{307}, Leu^{309}, Asn^{315}, Lys^{322}, Lys^{326}, Pro^{331}, Ser^{337}, Ala^{339}, Ala^{378}, and Lys^{414}.

A previous study elucidated the residues in murine IgG2b involved in binding to murine FcγRII (25). Of the residues investigated in that study, only N297A and E318A showed a complete abrogation of binding. Several other murine IgG2b residues exhibited more modest reduction in binding to FcγRII as follows: S239A, K248A, S267A, K322A, E333A, T335A, S337A, and K340A (25). Several of these residues also exhibited modest reduction in binding in the human system (*e.g.* S239A and T335A) or modest improvement in binding (*e.g.* K340A) but fell outside of the cut-off used in this study. Noteworthy differences between the two systems are as follows: D270A affecting only the human system, E318A affecting only the murine system, and K322A, S267A, and S337A exhibiting improved binding in the human system but slightly reduced binding in the murine.

In contrast to FcγRI, several variants exhibited improved binding to FcγRIIA and FcγRIIB (Classes 3–5). Of special interest are Class 4 containing residues which, when changed to Ala, improved binding only to FcγRII and Class 5 containing residues which, when changed to Ala, simultaneously improved binding to FcγRII and reduced binding to FcγRIIIA. These can be used to make IgG1 with improved specificity for FcγRII over FcγRIIIA.

Recently the crystal structures of human FcγRIIA (68) and FcγRIIB (69) have been solved. In the FcγRIIA report, it was suggested that in addition to the lower hinge (Leu^{234}–Gly^{237}), residues in IgG CH2 domain loops FG (residues 326–330) and BC (residues 265–271) might play a role in binding, although it was noted that these had yet to be demonstrated by mutagenesis. Of the four exposed residues in loop FG, A330Q had no effect, A327Q, A327S, and P329A reduced binding, and K326A improved binding. Of the five exposed residues in loop BC, two reduced binding when altered to Ala (D265A and D270A) and two improved binding (S267A and H268A). Several of the residues found to influence binding to FcγRII lie outside of the residues at the Fc:FcγRIIIA interface in the co-crystal structure (26). One of these, Asp^{280}, is not only distant from the Fc:FcγRIIIA interface but is distant from other FcγRII-influencing residues (Fig. 2*A*). However, both D280A and D280N improved binding to FcγRII, suggesting that this residue does indeed interact with FcγRII.

Human IgG1 Binding to Human FcγRIIIA—In addition to the Class 1 residues, positions that reduced binding to FcγRIIIA by 40% or more (when changed to Ala) are as follows: Ser^{239}, Ser^{267} (Gly only), His^{268}, Glu^{293}, Gln^{295}, Tyr^{296}, Arg^{301}, Val^{303}, Lys^{338}, and Asp^{376}. In the Fc crystal structure, these residues separate into two groups. Lys^{338} and Asp^{376} are at the CH2-CH3 interface and may affect the spatial relationship of these two domains, thereby affecting FcγRIIIA binding; note that changing these two residues did not significantly reduce binding to FcγRI, FcγRII, or FcRn. The other eight positions are clustered together near the Class 1 residues at the hinge-proximal end of the CH2 domain; of these, only Ser^{239}, Ser^{267}, and His^{268} were cited as part of the binding site in the Fc:FcγRIIIA crystal structure report (26). Of the remaining seven, a few might conceivably exert their effect by conformational change, *e.g.* Tyr^{296}, Arg^{301}, Val^{303}, Lys^{338}, and Asp^{376} (Fig. 2*B*). However, the Glu^{293} and Gln^{295} side chains are quite solvent-exposed, based on Fc crystal structures (30, 59), and are not involved in interactions which would hint at a conformational role. In addition to E293A reducing binding by 70% (Class 8), the more conservative change of E293D also showed a similar reduction (Table II) implying that Glu^{293} can indeed interact with FcγRIIIA.

Variants that improved binding to FcγRIIIA (Classes 3, 7, and 9) include T256A, K290A, S298A, E333A, K334A, and A339T. Of these, only Ser^{298} was cited as part of the binding site in the Fc:FcγRIIIA crystal structure report (26). Although Glu^{333} and Lys^{334} do not interact with FcγRIIIA in the co-crystal structure, their interaction with FcγRIIIA is supported by four lines of evidence. First, murine IgG2b E333A exhibited a modest reduction in binding to murine FcγRII (25). Although the same might not occur for murine FcγRIII, this shows that residues distant from the hinge region can influence binding to FcγR. Second, several non-Ala variants at Glu^{333} and Lys^{334} either improved or reduced binding to FcγRIIIA (Table II). Third, binding of E333A and K334A to FcγRIIIA-expressing CHO cells improved even more than seen in ELISA-based assays (Table VI). Finally, K334A exhibited a significant increase in ADCC. This increase in ADCC was additive when K334A was present with S298A and was further enhanced when E333A was present (Fig. 4).

Several residues that influenced binding, albeit modestly, to FcγRIIIA, FcγRIIA, and FcγRIIB, are located at the "bottom" of

the CH3 domain distant from the larger set of residues in the CH2 domain which exhibited a more pronounced effect on binding. Lys^{414} (Fig. 2A) showed a 40% reduction in binding for FcγRIIA and FcγRIIB (Class 6), Arg^{416} a 30% reduction for FcγRIIA and FcγRIIIA, Gln^{419} a 30% reduction to FcγRIIA and a 40% reduction to FcγRIIB, and Lys^{360} a 23% improvement to FcγRIIIA (Class 10). Taken together, their effect on binding of IgG1 to FcγRIIA, FcγRIIB, and FcγRIIIA suggests that the bottom of IgG1 may indeed be involved in the IgG1-FcγR interaction, although it may play only a minor role.

Human IgG1 Binding to Human FcRn—Previous studies have mapped the binding site of murine IgG for murine FcRn (13, 29, 70–74). These studies have implicated murine IgG residues Ile^{253}, His^{310}, Gln^{311}, His^{433}, Asn^{434}, His^{435}, and His^{436} as contacts for one FcRn molecule and Glu^{272} and His^{285} as contacts for a second FcRn molecule. In addition, the pH dependence of the IgG-FcRn interaction has been ascribed to His^{310} and His^{433} on IgG (as well as His^{250} and His^{251} on FcRn) (75).

In the current study of the human system, a larger number of residues were found that affected binding of IgG1 to human FcRn. Comparison of the human IgG1 sequence with the crystal structure of rat Fc bound to murine FcRn (29) shows that in the human Fc some of these residues could interact directly with human FcRn: Ile^{253}, Ser^{254}, Lys^{288}, Thr^{307}, Gln^{311}, Asn^{434}, and His^{435}. Near the Fc:FcRn interface in the crystal structure but not interacting directly are Arg^{255}, Thr^{256}, Asp^{312}, Glu^{380}, Glu^{382}, His^{433}, and Tyr^{436}. In the murine system it was found that altering Asn^{434} to Ala or Gln did not affect binding to murine FcRn (72, 74). However, in the human system N434A exhibited the largest improvement in binding seen for any single Ala substitution (Class 10) as well as showing additivity in combination variants (Table III). Note that whereas improvement in binding of the variants to FcRn occurred at pH 7.2 as well as at pH 6.0 (Table III), none of the variants bound well at pH 7.2. Hence, these single or combination variants may be useful in extending the half-life of human IgG1 in therapeutic antibodies, as previously found for murine IgG (13), and fulfill the requirement for binding at pH 6.0 and dissociating at pH 7.2.

Effect of Glycosylation—The presence of carbohydrate linked at residue Asn^{297} is required for binding to FcγR (25). In addition, the nature of the carbohydrate can influence binding (11, 12, 56, 57). In crystal structures of IgG (Fc and intact antibody), Asp^{265} interacts directly with the Asn^{297}-linked carbohydrate via hydrogen bonds (30, 59–61). Previous studies found that an D265A change in human IgG3 altered the composition of the Asn^{297}-linked carbohydrate and reduced binding to FcγRI (56, 57). In human IgG1, D265A (Class 1) the carbohydrate also differed from that of native IgG1 (Table IV), and binding to FcγRI was reduced. Variants at positions 258 and 301 also showed variation from native IgG1 and the other variants (Table IV). The two Arg^{301} variants exhibited an increase in binding to FcγRIIB, a decrease in binding to FcγRIIIA, and no effect on binding to FcγRI or FcRn (Class 5). D265A (Class 1) showed decreased binding to all FcγR, whereas E258A (Class 4) showed increased binding to FcγRII only. Hence, although it is possible that the idiosyncratic carbohydrate on these variants influenced binding rather than the amino acid changes directly affecting interaction with the FcγR, the data do not allow resolution of the two possibilities. For the Y296F, S298A, V303A, and K334A variants, there were no significant differences in carbohydrate from that of native IgG1 (Table IV). Hence the differences in binding to the various FcγR exhibited by these variants are unlikely to be the result of glycosylation differences.

Human IgG1 Binding to FcγRIIA and FcγRIIIA Polymorphic Forms—Human FcγRIIA has two known, naturally occurring allotypes that are determined by the amino acid at position 131 (52). Among the human IgG1 variants tested against both FcγRIIA-Arg^{131} and FcγRIIA-His^{131}, variants S267A, S267G, H268A, and D270 could discriminate between the polymorphic forms. This suggests that these IgG1 residues interact with FcγRIIA in the vicinity of FcγRIIA residue 131, and in the IgG1 Fc:FcγRIIIA crystal structure (26), Ser^{267} is adjacent to His^{131}.

Human FcγRIIIA has naturally occurring allotypes at position 48 (Leu, His, or Arg) and at position 158 (Val or Phe). The FcγRIIIA-Val^{158} allotype binds human IgG better than the FcγRIIIA-Phe^{158} allotype (45, 76), and this difference is reiterated in the ELISA format, cell-based, and ADCC assays in this study. The IgG1 Fc:FcγRIIIA crystal structure offers an explanation for this difference. In the crystal structure, Val^{158} interacts with the IgG1 lower hinge near Leu^{235}–Gly^{236} and with the FcγRIIIA Trp^{87} side chain (which in turn interacts with the important IgG1 Pro^{329}); introduction of the larger Phe^{158} may alter either or both of these interactions and thereby reduce the binding.

Some of the IgG1 variants exhibited better binding to FcγRIIIA-Phe^{158} (*e.g.* Classes 7 and 9) and could be further improved by combining individual variants (Table III). These same variants showed no improvement or minimal improvement in binding to FcγRIIIA-Val^{158} in the ELISA format assay. However, when tested on cells expressing FcγRIIIA-Val^{158} or in ADCC assays using FcγRIIIA-Val^{158}/Val^{158} donors, some of these variants did show superior interaction compared with native IgG1 (Table VI and Fig. 4). Comparing the ADCC results of select IgG1 variants with better binding to FcγRIIIA, the variants exhibited a significant improvement in ADCC for both FcγRIIIA-Phe^{158}/Phe^{158} and FcγRIIIA-Val^{158}/Val^{158} donors (Fig. 4). Indeed, using the S298A/E333A/K334A variant, the FcγRIIIA-Phe^{158}/Phe^{158} donor ADCC could be increased over 100% (*i.e.* >2-fold) compared with native IgG1 (Fig. 4C).

Although the influence of FcγRIIA polymorphic forms in various human diseases has been investigated for many years (reviewed in Ref. 77), the possible correlation between FcγRIIIA polymorphic forms and human disease has only recently been investigated (76, 78, 79). Given the possible involvement of FcγR in the mechanism of action of therapeutic antibodies (4–6), human IgG1 variants with improved binding capacity to human FcγR, especially variants with better binding to FcγRIIIA and simultaneous abrogation of binding to the inhibitory FcγRIIB, could be used to provide more efficacious therapeutic antibodies. In addition, a recent report on the occurrence of polymorphic FcγR forms in control populations showed that the FcγRIIIA-Phe^{158} allele is more prevalent than the FcγRIIIA-Val^{158} allele (77). Since the FcγRIIIA-Phe^{158} receptor binds human IgG1 less well than the FcγRIIIA-Val^{158} receptor, therapeutic antibodies with variant Fc portions that improve binding to FcγRIIIA-Phe^{158} at least to the level seen for FcγRIIIA-Val^{158} (if not more so) could provide increased therapeutic efficacy to the majority of the population.

Acknowledgments—We thank Dr. Jeffrey V. Ravetch (Rockefeller University) for valuable discussion concerning this study and the role of FcγR and Lori O'Connell for help in DNA sequencing and protein expression/purification.

REFERENCES

1. King, D. J., and Adair, J. R. (1999) *Curr. Opin. Drug Discovery Dev.* **2**, 110–117
2. Vaswani, S. K., and Hamilton, R. G. (1998) *Ann. Allergy Asthma Immunol.* **81**, 105–119
3. Holliger, P., and Hoogenboom, H. (1998) *Nat. Biotechnol.* **16**, 1015–1016
4. Clynes, R. A., Towers, T. L., Presta, L. G., and Ravetch, J. V. (2000) *Nat. Med.* **6**, 443–446
5. Clynes, R., Takechi, Y., Moroi, Y., Houghton, A., and Ravetch, J. V. (1998) *Proc. Natl. Acad. Sci. U. S. A.* **95**, 652–656

6. Anderson, D. R., Grillo-Lopez, A., Varns, C., Chambers, K. S., and Hanna, N. (1997) *Biochem. Soc. Trans.* **25,** 705–708
7. Armour, K. L., Clark, M. R., Hadley, A. G., and Williamson, L. M. (1999) *Eur. J. Immunol.* **29,** 2613–2624
8. Duncan, A. R., Woof, J. M., Partridge, L. J., Burton, D. R., and Winter, G. (1988) *Nature* **332,** 563–564
9. Weiner, L. M., Alpaugh, R. K., and von Mehren, M. (1997) *Cancer Immunol. Immunother.* **45,** 190–192
10. Peng, L. S., Penichet, M. L., and Morrison, S. L. (1999) *J. Immunol.* **163,** 250–258
11. Uma-a, P., Jean-Mairet, J., Moudry, R., Amstutz, H., and Bailey, J. E. (1999) *Nat. Biotechnol.* **17,** 176–180
12. Lifely, M. R., Hale, C., Royce, S., Keen, M. J., and Phillips, J. (1995) *Glycobiology* **5,** 813–822
13. Ghetie, V., Popov, S., Borvak, J., Radu, C., Matesoi, D., Medesan, C., Ober, R. J., and Ward, E. S. (1997) *Nat. Biotechnol.* **15,** 637–640
14. Gessner, J. E., Heiken, H., Tamm, A., and Schmidt, R. E. (1998) *Ann. Hematol.* **76,** 231–248
15. Gavin, A., Hulett, M., and Hogarth, P. M. (1998) in *The Immunoglobulin Receptors and Their Physiological and Pathological Roles in Immunity* (van de Winkel, J. G. J., and Hogarth, P. M., eds) pp. 11–35, Kluwer Academic Publishers Group, Dordrecht, The Netherlands
16. Sautes, C. (1997) in *Cell-mediated Effects of Immunoglobulins* (Fridman, W. H. and Sautes, C., eds) pp. 29–66, R. G. Landes Co., Austin, TX
17. Da'ron, M. (1997) *Annu. Rev. Immunol.* **15,** 203–234
18. Kabat, E. A., Wu, T. T., Perry, H. M., Gottesman, K. S., and Foeller, C. (1991) *Sequences of Proteins of Immunological Interest,* 5th Ed., United States Public Health Service, National Institutes of Health, Bethesda
19. Canfield, S. M., and Morrison, S. L. (1991) *J. Exp. Med.* **173,** 1483–1491
20. Chappel, M. S., Isenman, D. E., Everett, M., Xu, Y.-Y., Dorrington, K. J., and Klein, M. H. (1991) *Proc. Natl. Acad. Sci. U. S. A.* **88,** 9036–9040
21. Woof, J. M., Partridge, L. J., Jefferis, R., and Burton, D. R. (1986) *Mol. Immunol.* **23,** 319–330
22. Wines, B. D., Powell, M. S., Parren, P. W. H. I., Barnes, N., and Hogarth, P. M. (2000) *J. Immunol.* **164,** 5313–5318
23. Sarmay, G., Benzcur, M., Petranyi, G., Klein, E., Kahn, M., Stanworth, D. R., and Gergely, J. (1984) *Mol. Immunol.* **21,** 43–51
24. Gergely, J., Sandor, M., Sarmay, G., and Uher, F. (1984) *Biochem. Soc. Trans.* **12,** 739–743
25. Lund, J., Pound, J. D., Jones, P. T., Duncan, A. R., Bentley, T., Goodall, M., Levine, B. A., Jefferis, R., and Winter, G. (1992) *Mol. Immunol.* **29,** 53–59
26. Sondermann, P., Huber, R., Oosthuizen, V., and Jacob, U. (2000) *Nature* **406,** 267–273
27. Raghavan, M., and Bjorkman, P. J. (1996) *Annu. Rev. Cell Dev. Biol.* **12,** 181–220
28. Ward, E. S., and Ghetie, V. (1995) *Ther. Immunol.* **2,** 77–94
29. Burmeister, W. P., Huber, A. H., and Bjorkman, P. J. (1994) *Nature* **372,** 379–383
30. Deisenhofer, J. (1981) *Biochemistry* **20,** 2361–2370
31. Kunkel, T. P. (1985) *Proc. Natl. Acad. Sci. U. S. A.* **82,** 488–492
32. Lennon, G. G., Auffray, C., Polymeropoulos, M., and Soares, M. B. (1996) *Genomics* **33,** 151–152
33. Eaton, D. L., Wood, W. I., Eaton, D., Hass, P. E., Hollingshead, P., Wion, K., Mather, J., Lawn, R. M., Vehar, G. A., and Gorman, C. (1986) *Biochemistry* **25,** 8343–8347
34. Gorman, C. M., Gies, D. R., and McCray, G. (1990) *DNA Protein Eng. Tech.* **2,** 3–10
35. Presta, L. G., Lahr, S. J., Shields, R. L., Porter, J. P., Gorman, C. M., and Jardieu, P. M. (1993) *J. Immunol.* **151,** 2623–2632
36. Liu, J., Lester, P., Builder, S., and Shire, S. J. (1995) *Biochemistry* **34,** 10474–10482
37. Nilsson, K., Bennich, H., Johansson, S. G. O., and Ponten, J. (1970) *Clin. Exp. Immunol.* **7,** 477–489
38. Tsuchiya, S., Yamabe, M., Yamaguchi, Y., Kobayashi, Y., Konno, T., and Tada, K. (1980) *Int. J. Cancer* **26,** 171–176
39. Lucas, B., Giere, L., DeMarco, R., Shen, A., Chisholm, V., and Crowley, C. (1996) *Nucleic Acids Res.* **24,** 1774–1779
40. Meng, Y. G., Liang, J., Wong, W. L., and Chisholm, V. (2000) *Gene (Amst.)* **242,** 201–207
41. Papac, D. I., Briggs, J. B., Chin, E. T., and Jones, A. J. S. (1998) *Glycobiology* **8,** 445–454
42. Papac, D. I., Wong, A., and Jones, A. J. S. (1996) *Anal. Chem.* **68,** 3215–3223
43. Hudziak, R. M., Lewis, G. D., Winget, M., Fendly, B. M., Shepard, H. M., and Ullrich, A. (1989) *Mol. Cell. Biol.* **9,** 1165–1172
44. Carter, P., Presta, L., Gorman, C. M., Ridgway, J. B. B., Henner, D., Wong, W. L. T., Rowland, A. M., Kotts, C., Carver, M. E., and Shepard, M. H. (1992) *Proc. Natl. Acad. Sci. U. S. A.* **89,** 4285–4291
45. Koene, H. R., Kleijer, M., Algra, J., Roos, D., von dem Borne, E. G. K., and de Hass, M. (1997) *Blood* **90,** 1109–1114
46. Hogarth, P. M., Ierino, F. L., and Hulett, M. D. (1994) *Immunomethods* **4,** 17–24
47. van den Herik-Oudijk, I. E., Westerdaal, N. A. C., Henriquez, N. V., Capel, P. J. A., and van de Winkel, J. G. J. (1994) *J. Immunol.* **152,** 574–584
48. Tamm, A., Kister, A., Nolte, K. U., Gessner, J. E., and Schmidt, R. E. (1996) *J. Biol. Chem.* **271,** 3659–3666
49. Tax, W. J. M., Hermes, F. F. M., Willems, R. W., Capel, P. J. A., and Koene, R. A. P. (1984) *J. Immunol.* **133,** 1185–1189
50. Huizinga, T. W. J., Kerst, M., Nuyens, J. H., Vlug, A., von dem Borne, A. E. G. K., Roos, D., and Tetteroo, P. A. T. (1989) *J. Immunol.* **142,** 2359–2364
51. Presta, L. G., Chen, H., O'Connor, S. J., Chisholm, V., Meng, Y. G., Krummen, L., Winkler, M., and Ferrara, N. (1997) *Cancer Res.* **57,** 4593–4599
52. Clark, M. R., Clarkson, S. B., Ory, P. A., Stollman, N., and Goldstein, I. M. (1989) *J. Immunol.* **143,** 1731–1734
53. Sarmay, G., Lund, J., Rozsnyay, Z., Gergely, J., and Jefferis, R. (1992) *Mol. Immunol.* **29,** 633–639
54. Jefferis, R., Lund, J., and Pound, J. (1990) *Mol. Immunol.* **27,** 1237–1240
55. Idusogie, E. E., Presta, L. G., Gazzano-Santoro, H., Totpal, K., Wong, P. Y., Ultsch, M., Meng, Y. G., and Mulkerrin, M. G. (2000) *J. Immunol.* **164,** 4178–4184
56. Lund, J., Takahashi, N., Pound, J. D., Goodall, M., and Jefferis, R. (1996) *J. Immunol.* **157,** 4963–4969
57. Lund, J., Takahashi, N., Pound, J. D., Goodall, M., Nakagawa, H., and Jefferis, R. (1995) *FASEB. J.* **9,** 115–119
58. Capon, D. J., Chamow, S. M., Mordenti, J., Marsters, S. A., Gregory, T., Mitsuya, H., Byrn, R. A., Lucas, C., Wurm, F. M., Groopman, J. E., Broder, S., and Smith, D. H. (1989) *Nature* **337,** 525–531
59. Guddat, L. W., Herron, J. N., and Edmundson, A. B. (1993) *Proc. Natl. Acad. Sci. U. S. A.* **90,** 4271–4275
60. Harris, L. J., Skaletsky, E., and McPherson, A. (1998) *J. Mol. Biol.* **275,** 861–872
61. Harris, L. J., Larson, S. B., Hasel, K. W., and McPherson, A. (1997) *Biochemistry* **36,** 1581–1597
62. Chappel, M. S., Isenman, D. E., Oomen, R., Xu, Y. Y., and Klein, M. H. (1993) *J. Biol. Chem.* **268,** 25124–25131
63. Miller, K. L., Duchemin, A.-M., and Anderson, C. L. (1996) *J. Exp. Med.* **183,** 2227–2233
64. Burton, D. R., Jefferis, R., Partridge, L. J., and Woof, J. M. (1988) *Mol. Immunol.* **25,** 1175–1181
65. Hulett, M. D., Osman, N., McKenzie, I. F. C., and Hogarth, P. M. (1991) *J. Immunol.* **147,** 1863–1868
66. Porges, A. J., Redecha, P. B., Doebele, R., Pan, L. C., Salmon, J. E., and Kimberly, R. P. (1992) *J. Clin. Invest.* **90,** 2101–2109
67. Haagen, I. A., Geerars, A. J., Clark, M. R., and van de Winkel, J. G. (1995) *J. Immunol.* **154,** 1852–1860
68. Maxwell, K. F., Powell, M. S., Hulett, M. D., Barton, P. A., McKenzie, I. F. C., Garrett, T. P. J., and Hogarth, P. M. (1999) *Nat. Struct. Biol.* **6,** 437–442
69. Sondermann, P., Huber, R., and Jacob, U. (1999) *EMBO J.* **18,** 1095–1103
70. Kim, J.-K., Tsen, M.-F., Ghetie, V., and Ward, E. S. (1994) *Eur. J. Immunol.* **24,** 542–548
71. Kim, J.-K., Tsen, M.-F., Ghetie, V., and Ward, E. S. (1994) *Eur. J. Immunol.* **24,** 2429–2434
72. Ghetie, V., and Ward, E. S. (1997) *Immunol. Today* **18,** 592–598
73. Kim, J.-K., Tsen, M. F., Ghetie, V., and Ward, E. S. (1994) *Scand. J. Immunol.* **40,** 457–465
74. Medesan, C., Matesoi, D., Radu, C., Ghetie, V., and Ward, E. S. (1997) *J. Immunol.* **158,** 2211–2217
75. Raghavan, M., Bonagura, V. R., Morrison, S. L., and Bjorkman, P. J. (1995) *Biochemistry* **34,** 14649–14657
76. Wu, J., Edberg, J. C., Redecha, P. B., Bansal, V., Guyre, P. M., Coleman, K., Salmon, J. E., and Kimberly, R. P. (1997) *J. Clin. Invest.* **100,** 1059–1070
77. Lehrnbecher, T., Foster, C. B., Zhu, S., Leitman, S. F., Goldin, L. R., Huppi, K., and Chanock, S. J. (1999) *Blood* **94,** 4220–4232
78. Lehrnbecher, T., Foster, C. B., Zhu, S., Venzon, D., Steinberg, S. M., Wyvill, K., Metcalf, J. A., Cohen, S. S., Kovacs, J., Yarchoan, R., Blauvelt, A., and Chanock, S. J. (2000) *Blood* **95,** 2386–2390
79. Nieto, A., Caliz, R., Pascual, M., Mataran, L., Garcia, S., and Martin, J. (2000) *Arthritis & Rheum.* **43,** 735–739